NAVAL POSTGRADUATE SCHOOL

MONTEREY, CALIFORNIA

THESIS

DIRECTIONAL CHARACTERISTICS OF INNER SHELF INTERNAL TIDES

by

Kendra Leigh Crabbe

June 2007

Thesis Advisor:	Timothy P. Stanton
Second Reader:	William J. Shaw

Approved for public release; distribution is unlimited.

THIS PAGE INTENTIONALLY LEFT BLANK

REPORT DOCUMENTATION PAGE		*Form Approved OMB No. 0704-0188*
Public reporting burden for this collection of information is estimated to average 1 hour per response, including the time for reviewing instruction, searching existing data sources, gathering and maintaining the data needed, and completing and reviewing the collection of information. Send comments regarding this burden estimate or any other aspect of this collection of information, including suggestions for reducing this burden, to Washington headquarters Services, Directorate for Information Operations and Reports, 1215 Jefferson Davis Highway, Suite 1204, Arlington, VA 22202-4302, and to the Office of Management and Budget, Paperwork Reduction Project (0704-0188) Washington DC 20503.		

1. AGENCY USE ONLY *(Leave blank)*	2. REPORT DATE June 2007	3. REPORT TYPE AND DATES COVERED Master's Thesis	
4. TITLE AND SUBTITLE Directional Characteristics of Inner Shelf Internal Tides		5. FUNDING NUMBERS **Partial N0001407WR20220**	
6. AUTHOR(S) Kendra Leigh Crabbe			
7. PERFORMING ORGANIZATION NAME(S) AND ADDRESS(ES) Naval Postgraduate School Monterey, CA 93943-5000		8. PERFORMING ORGANIZATION REPORT NUMBER **N/A**	
9. SPONSORING /MONITORING AGENCY NAME(S) AND ADDRESS(ES) ONR, Physical Oceanography		10. SPONSORING/MONITORING AGENCY REPORT NUMBER **N/A**	
11. SUPPLEMENTARY NOTES The views expressed in this thesis are those of the author and do not reflect the official policy or position of the Department of Defense or the U.S. Government.			
12a. DISTRIBUTION / AVAILABILITY STATEMENT Approved for public release, distribution is unlimited.		12b. DISTRIBUTION CODE A	

13. ABSTRACT (maximum 200 words)

Internal tidal bore events observed at a Monterey Bay inner shelf site are analyzed. A six month data set from the Naval Postgraduate School Monterey Inner Shelf Observatory site included water column current velocities and thermal structure data. Isothermal displacements paired with concurrent velocity observations in the water column were used to assess the events' individual characteristics as the internal tidal bores shoal and approach the surf zone. The primary hypothesis tested was that if the internal tidal bores observed at MISO had strong along-shore current velocity signatures, then those bores were most likely generated at the Monterey Bay Submarine Canyon edge or were evidence of an internal edge wave. If velocity signatures were primarily cross-shore, then bores would most likely propagate from straight across the shelf westward from their generation site at the continental shelf break. Visual observations of temperature profiles, current vector plots, linear regressions, and histograms were employed to test the relationships between forcing, stratification, and internal tidal bore forms. The unique aspect of this research is the focus on shoaling effects of internal tidal bores after they have traversed the continental shelf and impinge on the nearshore. Additionally, coastlines with significant bathymetric features, like Monterey Bay, are of operational interest to the military and are prime generation sites for these internal bore and soliton events. Internal tidal bores can directly impact naval special operations; specifically, amphibious landings and SEAL Delivery Vehicle operations. Understanding where and how bore and soliton events are generated is beneficial to nearshore modelers and operators.

14. SUBJECT TERMS Internal tidal bore, soliton, solibore			15. NUMBER OF PAGES 94
			16. PRICE CODE
17. SECURITY CLASSIFICATION OF REPORT Unclassified	18. SECURITY CLASSIFICATION OF THIS PAGE Unclassified	19. SECURITY CLASSIFICATION OF ABSTRACT Unclassified	20. LIMITATION OF ABSTRACT UL

THIS PAGE INTENTIONALLY LEFT BLANK

DIRECTIONAL CHARACTERISTICS OF INNER SHELF INTERNAL TIDES

Kendra L. Crabbe
Ensign, United States Navy
Oceanography B.S., United States Naval Academy, 2006

Submitted in partial fulfillment of the
requirements for the degree of

MASTER OF SCIENCE IN PHYSICAL OCEANOGRAPHY

from the

NAVAL POSTGRADUATE SCHOOL
June 2007

Author: Kendra Leigh Crabbe

Approved by: Timothy P. Stanton
                 Thesis Advisor

                 William J. Shaw
                 Second Reader

                 Mary L. Batteen
                 Chairman, Department of Oceanography

iii

THIS PAGE INTENTIONALLY LEFT BLANK

ABSTRACT

Internal tidal bore events observed at a Monterey Bay inner shelf site are analyzed. A six month data set from the Naval Postgraduate School Monterey Inner Shelf Observatory site included water column current velocities and thermal structure data. Isothermal displacements paired with concurrent velocity observations in the water column were used to assess the events' individual characteristics as the internal tidal bores shoal and approach the surf zone. The primary hypothesis tested was that if the internal tidal bores observed at MISO had strong along-shore current velocity signatures, then those bores were most likely generated at the Monterey Bay Submarine Canyon edge or were evidence of an internal edge wave. If velocity signatures were primarily cross-shore, then bores would most likely propagate from straight across the shelf westward from their generation site at the continental shelf break. Visual observations of temperature profiles, current vector plots, linear regressions, and histograms were employed to test the relationships between forcing, stratification, and internal tidal bore forms. The unique aspect of this research is the focus on shoaling effects of internal tidal bores after they have traversed the continental shelf and impinge on the nearshore. Additionally, coastlines with significant bathymetric features, like Monterey Bay, are of operational interest to the military and are prime generation sites for these internal bore and soliton events. Internal tidal bores can directly impact naval special operations; specifically, amphibious landings and SEAL Delivery Vehicle operations. Understanding where and how bore and soliton events are generated is beneficial to nearshore modelers and operators.

THIS PAGE INTENTIONALLY LEFT BLANK

TABLE OF CONTENTS

viii

LIST OF FIGURES

LIST OF TABLES

THIS PAGE INTENTIONALLY LEFT BLANK

ACKNOWLEDGMENTS

THIS PAGE INTENTIONALLY LEFT BLANK

I. INTRODUCTION

Nonlinear solitary internal waves, or solitons, were first observed in 1834 as surface disturbances propagating through a channel (Stanton and Ostrovsky 1998). When solitons or the wave envelopes that encompass them (bores) are tidally forced, these typically strongly non-linear internal wave events are named internal tides. Nonlinear coastal internal tides impact several scientific areas including ocean acoustic propagation, cross-shore transport on the shelf, biological oceanography, and coastal engineering (Farmer and Armi 1999). Most recently, naval forces around the world, particularly submarine forces, have demonstrated interest in understanding and predicting coastal, tide-forced internal tide activity. Despite the interest, few studies have been completed to assess the impact of internal tides on the inner continental shelf. Equipped with knowledge regarding non-linear internal tide directionality and shoaling effects, naval officers, scientists, and coastal industrialists will be able to improve the safety for shallow water special forces and improve the skill of high resolution environmental models.

A. INTERNAL TIDES

1. Definition and Generation

Internal waves (IW) are water particle disturbances that are supported by density gradients within the ocean. Internal tides are IW that are forced by the barotropic tides. The amplitude of the internal tide is highly dependent on water column stratification and the strength of forcing, with strong internal tides in coastal regions being seen as primarily mode 1 waves (Ray 2001).

A commonly observed generation mechanism for internal tides is the lee-wave mechanism (Apel et al. 1985). In this case ebb tidal flow over a bottom feature or shelf break generates a steepening dip in the pycnocline. The isopycnal depression forms a steep-edged bore that propagates shoreward during the slack tide (Figure 1). Wave dispersion and strong non-linearity cause wave degeneration into solitons. Internal waves may also be generated from the relaxation of internal hydraulic flows, intrusions created by mixed layer collapse, or upstream influence (Farmer and Armi 1999).
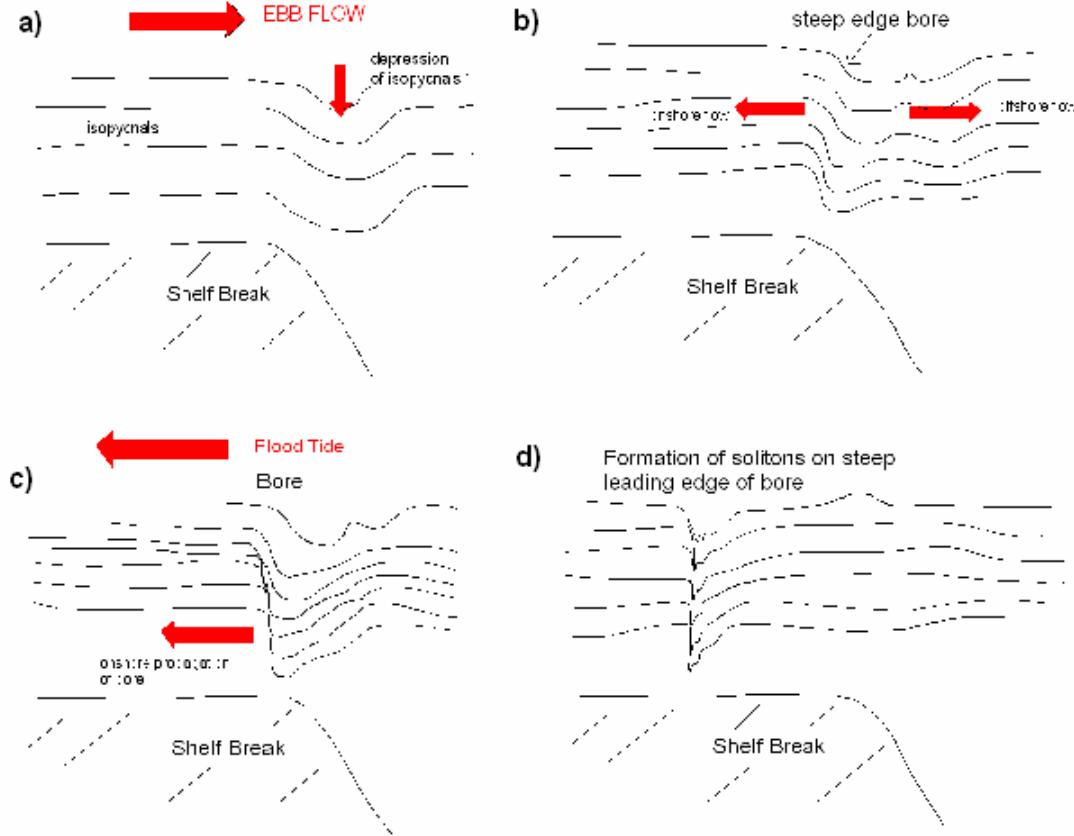
Figure 1.   Internal tidal bore and soliton generation by the lee wave mechanism. (a) A depression in the pycnocline results from tidal waters ebbing across the shelf break. (b) A steep-edged shoreward-propagating bore forms during slack tide. (c) Internal bore's shoreward propagation assisted by flood tide. (d) Steep leading edge of the bore degenerates into solitons through the process of wave dispersion. (After Holloway 1987)

2.   Bores and Solitons

As discussed above, steep edged internal bores move across the shelf, disperse, and disintegrate into groups, or packets, of waves that are commonly called solitons (Stanton and Ostrovsky 1998). Solitons can be characterized by large, rapid isopycnal displacements and strong upper layer shoreward current fluctuations. In this discussion, the term "internal tidal bore" (ITB) is used to describe the lower frequency density disturbances of the primary bore. "Solitons" or "soliton packet" is used to describe the higher frequency perturbations. Steep edged bores typically begin disintegrating into soliton packets so that both bores and solitons propagate inshore together in a phase-

2

locked manner. When propagating together, the internal bores and nonlinear internal solitary waves can be termed "solibore" events (Hosegood and van Haren 2004). Isotherm fluctuation depictions are highly useful for identifying bores, solitons, and solibores (Figure 2).
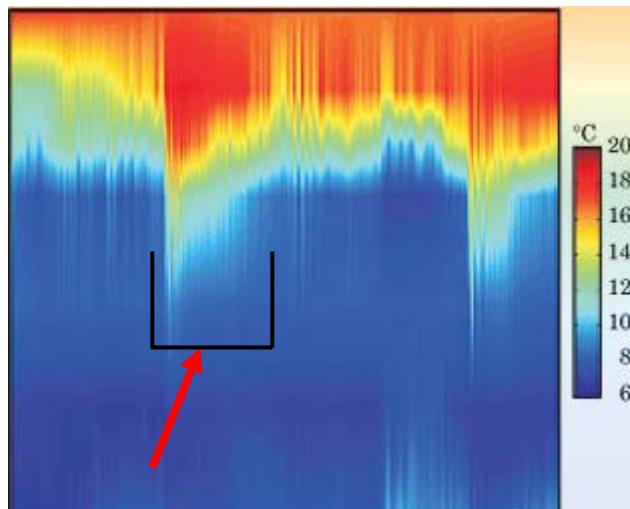
Figure 2.   Graphic depicting a "solibore." A solibore is a wave train that includes an internal tidal bore (the largest disturbance in the thermocline at the onset of the wave train marks the start of the event envelope) and solitons (high frequency spikes at the boundary of the upper and lower water layers near the bore's leading edge). The red arrow and brackets mark the extent of the internal tidal bore event. (From Kuperman and Lynch 2005)

Both bores and solitons are extremely nonlinear waves of a fairly permanent form (Garrett and Munk 1979) that are difficult to predict and measure. In areas of high activity, IW events including bore and soliton disturbances can result in surface "slicks" that can be viewed and studied through aircraft observation, satellite imagery, and ships' radar (Kropfli et al. 1999). Figure 3 is a radar image from an oceanographic ship in the South China Sea. In the image, surface slicks highlighted by radar indicate the location of internal waves beneath the ocean surface. The slicks are regions of surface convergence created by wave-induced water particle displacements. Figure 4 depicts the modulation of backscatter strength in convergence and divergence associated with IW events.

R70 ORI 2006 Jun04 0215L 21.07432500N 116.78609333E 3.42Kts HD 207.6   ROCOS-IONTU 1999 (C)
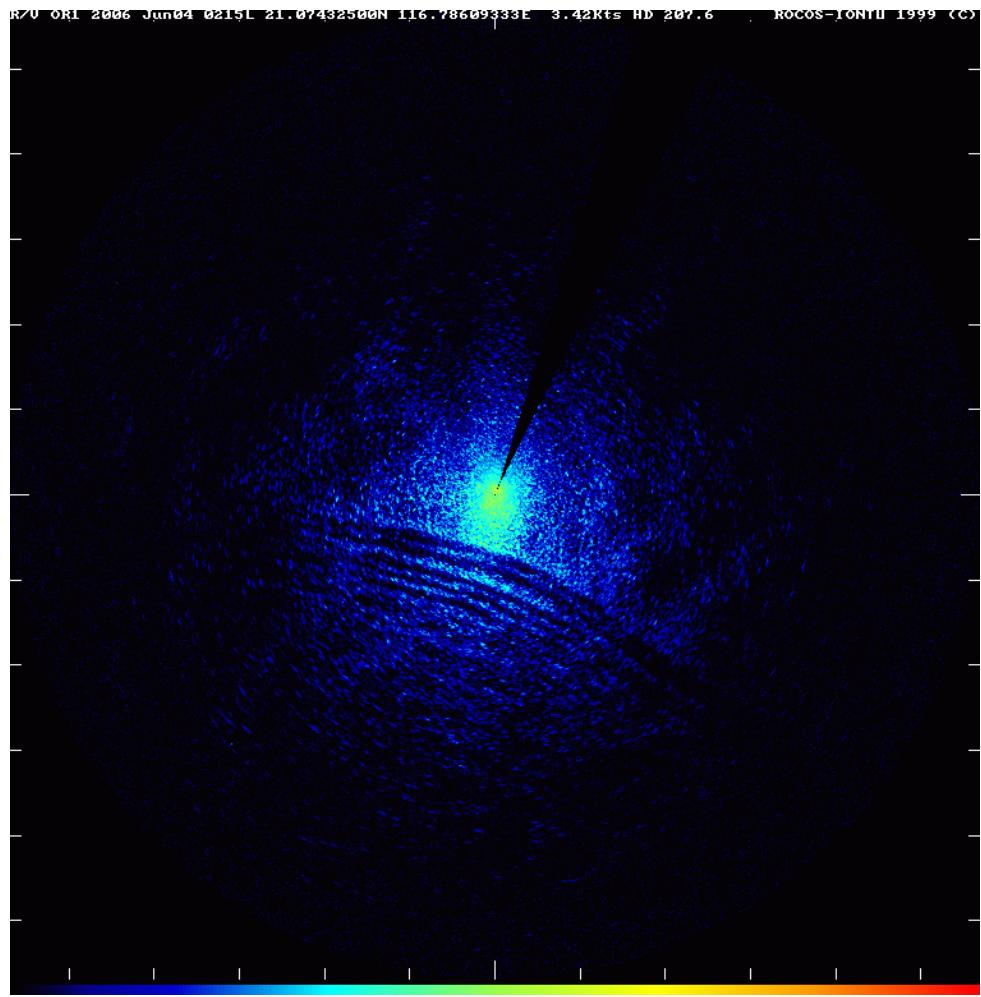
Figure 3.   Ship's radar image depicting surface slicks caused by internal waves. Provided courtesy of Dr. Steven Ramp and Fred Bahr, Naval Postgraduate School, Monterey, California.
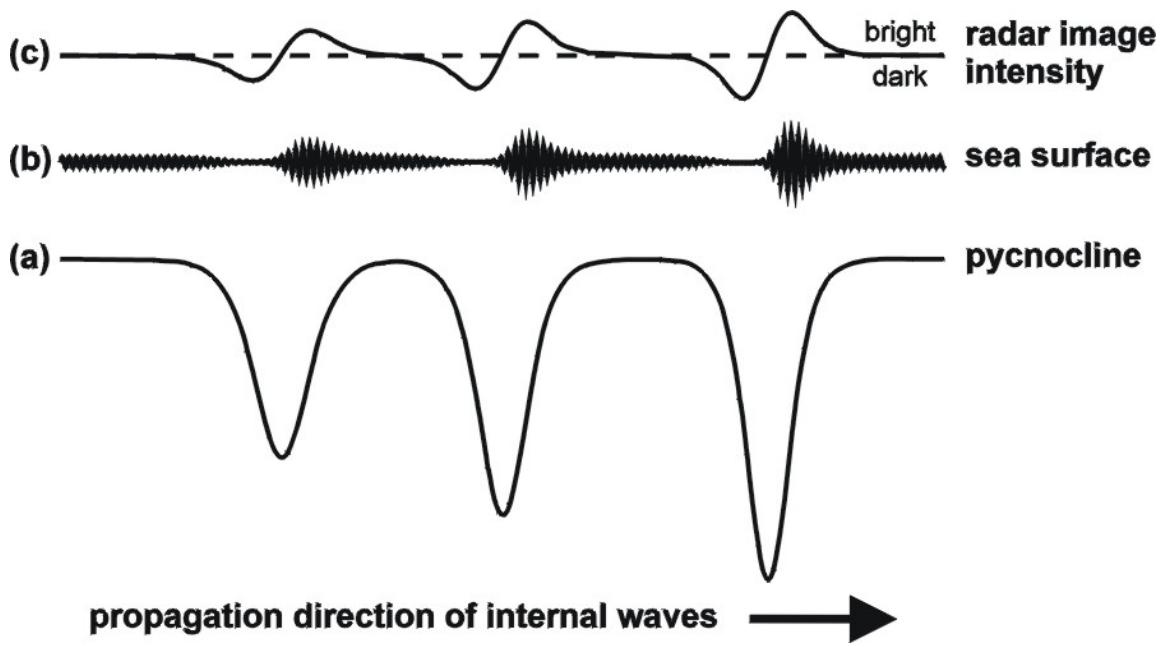
Figure 4.   Graphical description of internal wave detection using radar. Note that when using radar to identify an internal wave, the surface translation would be the brighter return while the end of the bore translates to the darker portion of the "slick." (From Alpers, et al. 2002)

3.   Prior Research and Modeling Efforts

Apel, et al. (1985) described large-amplitude internal soliton generation by intense tidal flow over sharp bathymetric features in the Sulu Sea using moored current meter arrays, thermistors, and remote sensing to investigate internal wave generation. Seventeen soliton packets were analyzed and compared to solitary-wave evolution theory. Apel, et al. noted that internal wave phase retardation and speed reduction occurred with distance and radial spreading. It was concluded that theoretical calculations of wave number, speed, and spacing were comparable to observations; however, amplitudes and widths depended on factors not currently described by theory.

Holloway (1987) studied internal solitons and their energy fluctuations near the Australian North West Shelf. Holloway observed that the steep leading face of the shoaling internal tide formed an internal hydraulic jump as it shoaled over the shelf slope

near the shelf break. He concluded that the hydraulic jumps and the soliton packets that sometimes follow them contributed significantly to the dissipation of the internal tide.

Petruncio (1998) published a study of observations of Monterey Bay Submarine Canyon's internal tides. Current velocity data from two shipboard experiments in 1994 revealed semidiurnal internal tidal currents an order of magnitude greater than estimated in Monterey Bay. He found that kinetic and potential energy was greatest along wave paths predicted by linear wave theory. Energy ratios were observed to be below estimates and attributable to topography constraints. Petruncio noted that internal tide behavior differed in April versus October because of varying stratification conditions and that dense water was vertically transported from within the Monterey Bay canyon up onto the shelf.

Stanton and Ostrovsky (1998) observed extremely non-linear internal tidal bores with series of leading edge internal solitons near the northern Oregon continental shelf. Their findings included a description of the highly nonlinear solitons that were observed on a shallow and very strongly stratified pycnocline during periods of strong tidal forcing. Stanton and Ostrovsky compared their observations to Korteveg-de Vries (KdV) equation results. They found that the next order model, the "CombKdV model" was more applicable to internal solitons found at the shelf because that model accounts for a higher degree of nonlinearity. The CombKdV equation was used to successfully reproduce the isopycnal displacements, widths, and amplitudes of the observed non-linear tidally forced internal solitons.

In 1999, Holloway and Merrifield published further analysis of internal tide generation mechanisms using modeling techniques. They used a fully three-dimensional nonlinear, free surface, hydrostatic, sigma coordinate, and primitive equation model with varying topographic inputs. Holloway and Merrifield concluded that critical shelf and topographic feature slopes are important for internal tide generation while depth of a topographic feature is less significant. Additionally, they found that ridges consistently produced much more energetic internal tides than did similar-sized sea mounts.

Because understanding internal tide generation was the first step in understanding the process as a whole, previous research and the associated conclusions have primarily

focused on generation. As interest in oceanographic processes over the inner shelf has become more important, the study of internal wave energy dissipation has become more common. Additionally, as the missions of naval forces around the world have shifted from the open ocean to the littoral region, interest in internal wave impact on acoustics and amphibious landings has increased. To date, the impact of internal waves on the inner shelf where shoaling and dissipation must be strong has not been significantly studied.

4. Environmental Impact

Oceanographers and environmentalists in Monterey and around the world are attempting to define the impact of internal tides on coastal environments and global climate. For over 75 years, it was thought that tidal energy dissipated almost entirely when seas experienced friction on continental shelves (Wunsch 2000). Wunsch concluded that frictional dissipation of tidal energy accounted for only a portion of the power needed to drive ocean mixing. Some scientists believe that internal tides may significantly contribute to energy dissipation, and, therefore, ocean mixing and global climate (Baines 1982, Munk 2001, Garrett 2003). Internal tide turbulence can generate upward nutrient transport spurring biological growth and transport which affects coastal fisheries. Furthermore, in locations with wide continental shelves and large tidal amplitude fluctuations, internal tides can be significant enough to affect offshore drilling operators and their equipment (Garrett 2003).

5. Naval Relevance

The United States Navy is interested in any type of information that can improve communication capabilities, establish theatre dominance, keep personnel safer, and maximize operational efficiency. As the navy increases focus on inter-service and inter-disciplinary operations, focus on research and development is increased. Meanwhile, the responsibility of employing power and spending wisely remains a priority for senior naval officers. Admiral Michael G. Mullen, USN, Chief of Naval Operations is quoted:

> I believe in the power and in the genius of industry in this country. We need good ideas. We need to stretch our imaginations. We need to be able to stay on top. But we can't afford every new gadget, we can't afford the "Star Wars" version of every new idea. We need to be selective and efficient. (Mullen 2007)

The highest ranking naval officer, Admiral Mullen, is communicating the necessity of intelligence and technological advancement in an efficient manner. In a time of war, the military of the United States of America must defend their people and their country's borders while maximizing resources and spending cautiously.

One of the navy's most useful platforms is the submarine. Submarines offer a stealthy and expedient method of intelligence gathering and weapons deployment. Submarines primarily rely on acoustics for self-defense which involves target detection, identification, tracking, and elimination. Internal tides rapidly and significantly affect ocean sound velocity fields and, therefore, the acoustic wave field. This, in turn, makes communications and object detection less reliable and more complicated. Having greater knowledge of internal tides and, therefore, the acoustic environment, could improve performance.

Another tactically useful naval platform is the SEAL (Sea-Air-Land teams) Delivery Vehicles (SDVs). It is often used in conjunction with submarines. SDVs have been deployed from specially crafted chambers within submarines to capitalize on covertness. The SDVs can then travel underwater for several miles to reach a target area. These small underwater vehicles travel in very shallow water where the passage of a strong internal tidal bore (ITB) event could push the vehicle into the ocean floor or expose the vehicle on the surface. SDVs can be difficult to control and to keep hidden if large amplitude current and density fluctuations occur due to an ITB. Additionally, ITBs are capable of re-suspending sediment which decreases visibility in the inner shelf region. These effects pose risk to the lives of personnel and the loss of covertness (Pike 2007). See Table 1 which displays the many meteorological and oceanographic conditions that threaten mission completion. Note that current velocities, wave heights, and water temperatures are listed as limiting environmental conditions. The presence of strong non-linear coastal internal tides pose an additional factor to be considered.

MET/OC ELEMENT	CRITICAL THRESHOLD	IMPACT ON OPERATIONS
Current	> 2.5 kts	Degradation of navigation/swimmer capabilities
Wave Height	> 3 ft combined seas	Launch and recovery
Tides	Low water < 8 ft Tidal range > 2 ft	Detectability/Navigation
Water Clarity	> 10 ft visibility from surface	Detectability
Water Temperature	50° - 60°F, wet suit < 50°F, dry suit	Diver degradation/Hypothermia
Lunar Illumination	Full moon, clear sky	Detectability
Bioluminescence	Any conditions that allow visible detection of an SDV submerged 10 ft in ambient light	Platform/swimmer detection

Table 1.   Meteorological and oceanographic conditions that limit SEAL delivery vehicle operations and SEAL team members' safety. Specifically, note that currents, wave heights, and water temperature are all significant factors. (Pike 2007).

Finally, many areas of military interest across the globe include shorelines with sharp shelf breaks that provide ITB generation sites. Some of these sites have significant riverine runoff which increases stratification and provides a medium for strong internal wave propagation to occur. These sites include the Taiwanese and Chinese coasts. Armed with knowledge of coastlines similar to Monterey Bay and the coastal processes associated with these coastlines, the United States military can more efficiently perform its mission and protect its people.

B.   EXPERIMENTAL SITE

1.   Monterey Bay

Monterey Bay, on the central California coast, is a good location for observing and analyzing internal tide activity found near continental slope breaks and areas of sloping irregular bathymetry. Monterey Bay has a classic continental shelf which is bisected by a deep submarine canyon in the middle of the bay, with associated ridges and a submarine fan. Figure 5 is a map of the Monterey Bay and details significant

bathymetric features and research sites. With an interesting and complex experimental field, scientists and researchers from many institutions have formed a coastal network of data-gathering partners including the Naval Postgraduate School, Monterey Bay Aquarium Research Institute (MBARI), Moss Landing Marine Labs, and the University of California at Santa Cruz (UCSC) among others. With a wealth of knowledge, experience, and equipment, the central and southern Californian coast provides many data sources for internal tide studies.
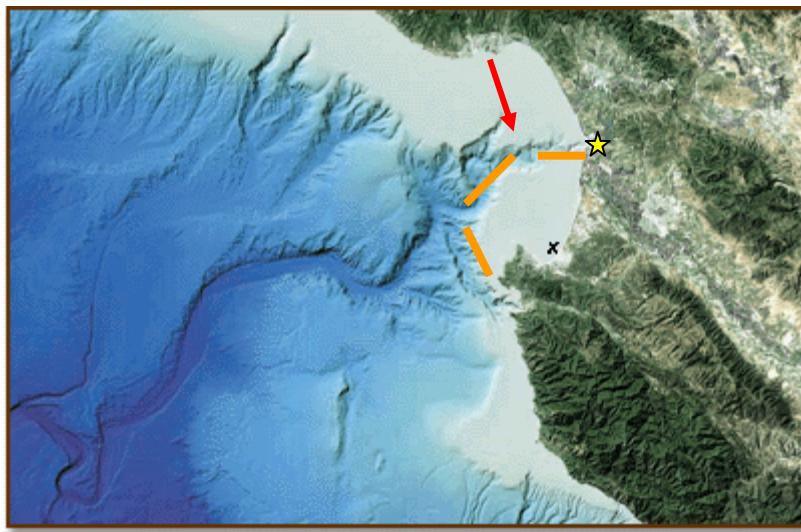
Figure 5. Map detailing Monterey Bay bathymetry. The red arrow points to the submarine canyon, the "x" represents the Monterey Inner Shelf Observatory (MISO) site, the star represents Monterey Bay Aquarium Research Institute (MBARI), and the orange lines mark the shelf break where internal waves are likely to occur and affect conditions at MISO. (From Tjoa 2003)

2. Offshore Observations

Monterey Bay's bathymetry provides sites for ITB generation, but the establishment of significant stratification is also necessary for the cross-shore propagation of internal tides. The Monterey Bay Aquarium Research Institute (MBARI) maintains data archives that have been useful for characterizing stratification across the Bay's shelf. Specifically important to this paper, data was gathered in 2006 using MBARI's Dorado Autonomous Underwater Vehicle (AUV). The AUV deployment was part of a field campaign named BIOLUME where conductivity, temperature, and depth (CTD) data was gathered as well as measurements of bioluminescence fluctuations (MBARI 2007). This

study used AUV tracks from portions of the BIOLUME project to estimate shelf stratification in the lower part of Monterey Bay nearest the Monterey Inner Shelf Observatory (MISO) site. Figure 6 shows AUV sampling tracks that began at the southern end of the Monterey Bay close to MISO, moved cross-shelf toward the long-term M2 mooring near the center of the bay, traversed to the northern portion of the bay, and then retraced a portion of the path before sampling along the submarine canyon. The first segment of the AUV deployment, near the MISO location to the M2 mooring, was used to assess shelf stratification.
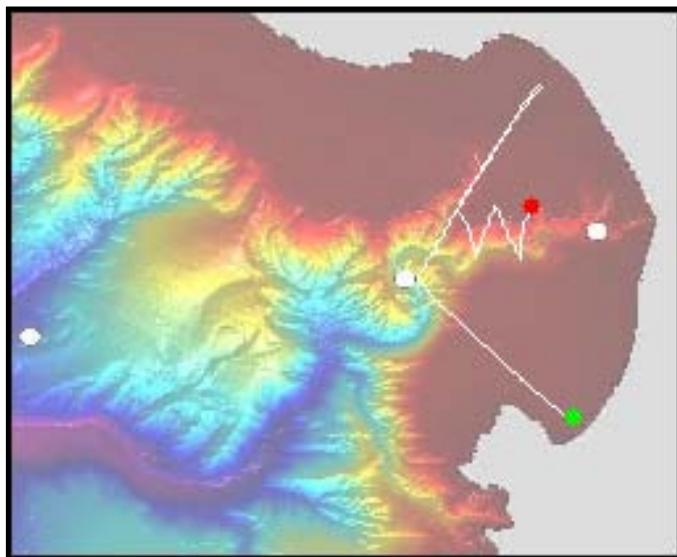
Figure 6.   Dorado AUV track for BIOLUME campaign. Green marker indicates AUV starting location. Red marker indicates finish. Note that AUV begins on-shelf near MISO and moves directly off-shelf. (From MBARI 2007)

C.   SHELF STRATIFICATION

Stratification in Monterey Bay varies seasonally. In the spring and summer, upwelling occurs which provides upward moving cool water from a depth of approximately 80 m. Summer stratification is stronger than winter stratification on the Monterey Bay shelf. In the summer, local heating warms the ocean surface, upwelling pushes cool water onto the shelf near the ocean floor, and near-surface stratification increases. These effects create an environment that can be approximated by a two-layer system (Tjoa 2003). Internal tide activity, specifically internal bore activity, is most likely to occur in a strongly stratified near two-layer system where buoyancy frequencies are high. Profiles of N^2, the buoyancy frequency (also Brunt Vaisala or stratification

frequency), vs. depth determine stratification strength. The buoyancy frequency,

$$N^2 = -\frac{g}{\rho} * \frac{\partial \rho}{\partial z},$$ represents the maximum vertical frequency excited by fluid parcel

vertical displacement. Surface stratification across the shelf and high buoyancy frequencies are necessary for the shoreward propagation of the internal tide into the coast.

1. Density and Buoyancy Frequency

Density and buoyancy frequency profiles generated from MBARI's Dorado AUV data were used to assess Monterey Bay shelf stratification during the late summer and fall of 2006. The stratification conditions at a mid-shelf position with 60 m depth over several AUV surveys are discussed below.

The profile from early August 2006, YD 214.2557 (Figure 7) had a shallow upper mixed layer which extended to ~ 12 m in depth with a relative difference between the upper and bottom layer densities of ~ .5 kg/m^3. The pycnocline extended from 12 – 15 m for an extent of ~3 m in depth. Stratification approximated a two-layer system, but was not strong throughout the water column because density did not fluctuate throughout the water column; instead, density was relatively constant from the surface to 12 m and from 15 m to the bed. From 12-15 m the buoyancy frequency was greatest.

In late August, YD 227.151, Figure 8, there was a poorly defined upper mixed layer that reached 10 m in depth. The pycnocline of this profile had a sharp interface from 10 – 11 m in depth. The bottom layer density increased very slowly with depth with a total density fluctuation of .5 kg/m^3 over ~ 60 m. The density difference between the upper and lower layers in this profile is ~ 1 kg/m^3 which could support ITB events.

In early September, YD 249.0992, Figure 9, no mixed layer was observed. The pycnocline appeared to begin near the surface and extended to ~ 9 m where a buoyancy frequency maximum occurred. The layer below the pycnocline slowly increased in density. The absence of a distinct upper layer or difference in the upper and lower layers of water indicates that stratification was weak and the propagation of internal tidal events could have been limited.

In late September, YD 270.0874, Figure 10, no upper level stratification is observable. A mixed layer extended from the surface to 44 m and varied in density by ~ .1 kg/m^3 over its entire extent. No distinct pycnocline was observed. Density increased slowly from 44 m to the bottom. Maximum buoyancy frequency and static stability values occurred just below the deep mixed layer because that area was the only area where a substantial density variation occurred. The maximum values were approximately two orders of magnitude less than those observed in August and early September. Internal tide propagation would have been limited in this environment.

In October 2006, YD 291.0824, Figure 11, the mixed layer extended to almost 28 m before a sharp pycnocline at ~ 10 m depth. In this case, maximum buoyancy frequency occurred at 29 m depth and was greater than the value seen in late September, but less than the maximum August values. The difference between upper and bottom layer density was ~ 1 kg/m^3. Internal wave propagation could have occurred in this environment; however, the propagation interface would have been deeper and any events would have been weaker than those in August.

Figure 12 displays density sections ranging from April to October. The time series of stratification show that on-shelf stratification was strongest in April, May, August, and early September of 2006. A thin shallow layer of low density water—deep blue in color—is separated from and on top of a thick deep layer of high density water—yellowish in color. Strong inner shelf stratification was present from April through early September and weakened by mid-September.
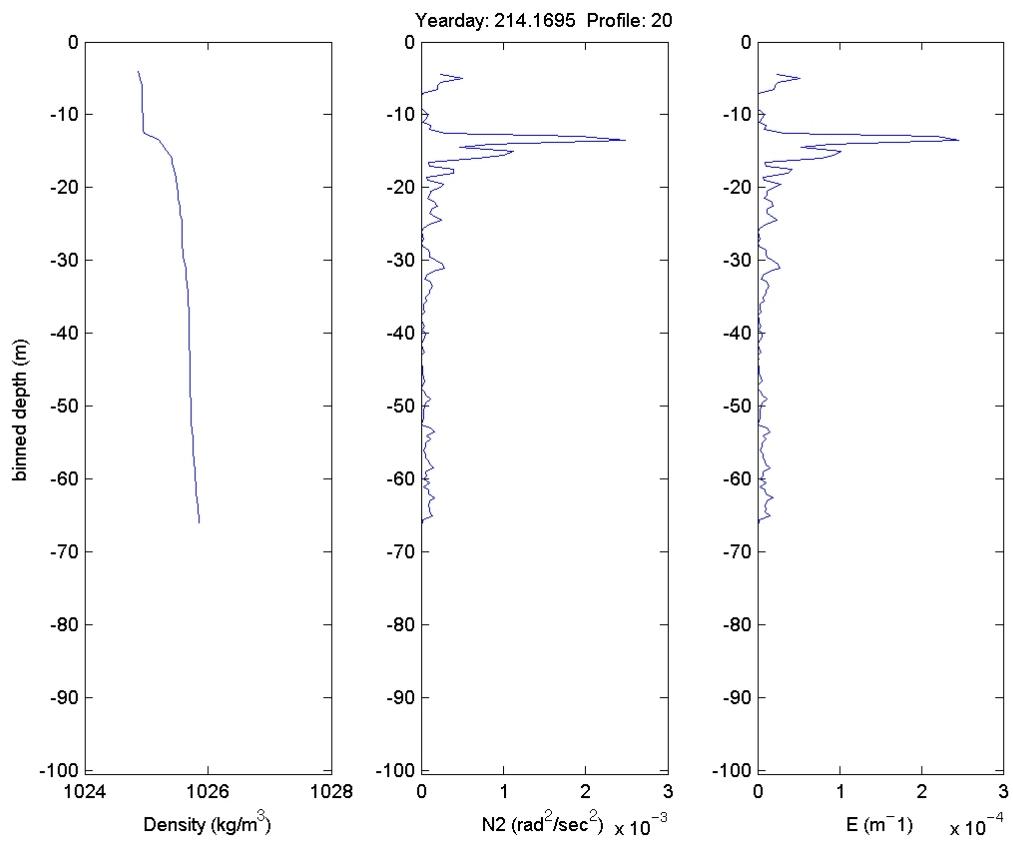
Figure 7.   YD 214.2557. Early August 2006. Profile 20, (left) Density vs. depth, (middle) N^2 vs. depth, (right) stability vs. depth.
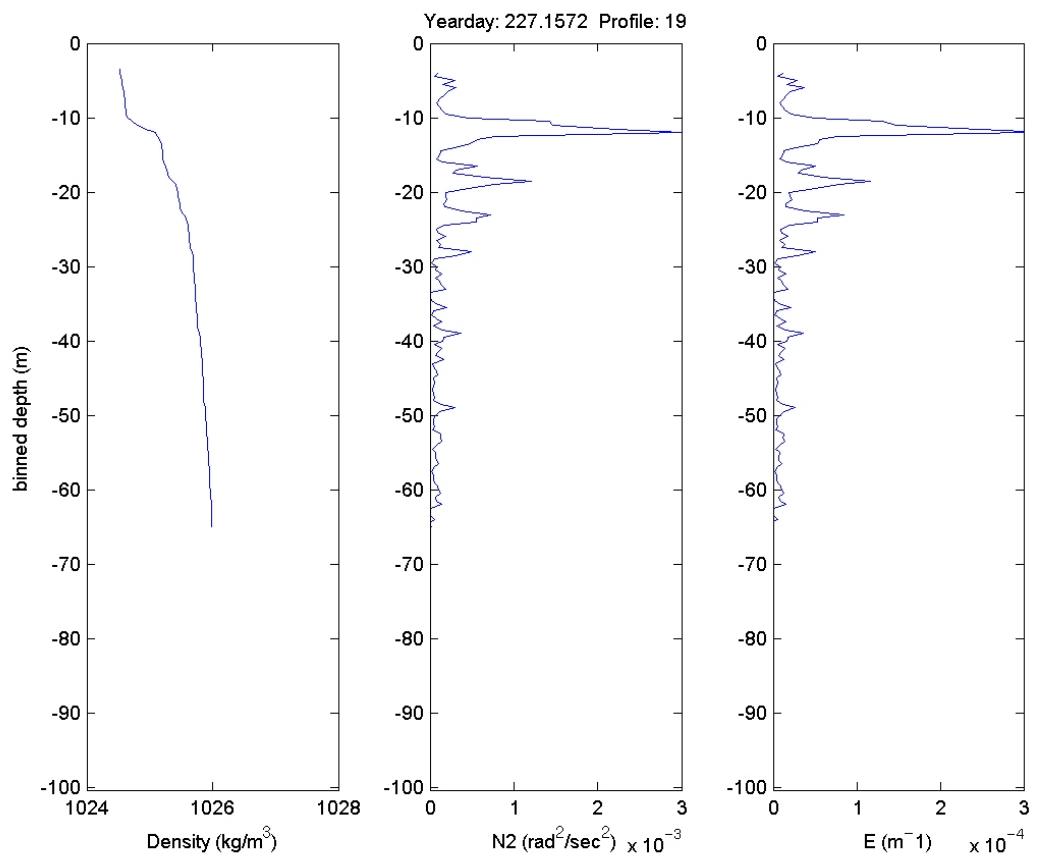
Figure 8.   YD 227.151. Late August 2006. Profile 19, (left) Density vs. depth, (middle) N^2 vs. depth, (right) stability vs. depth.
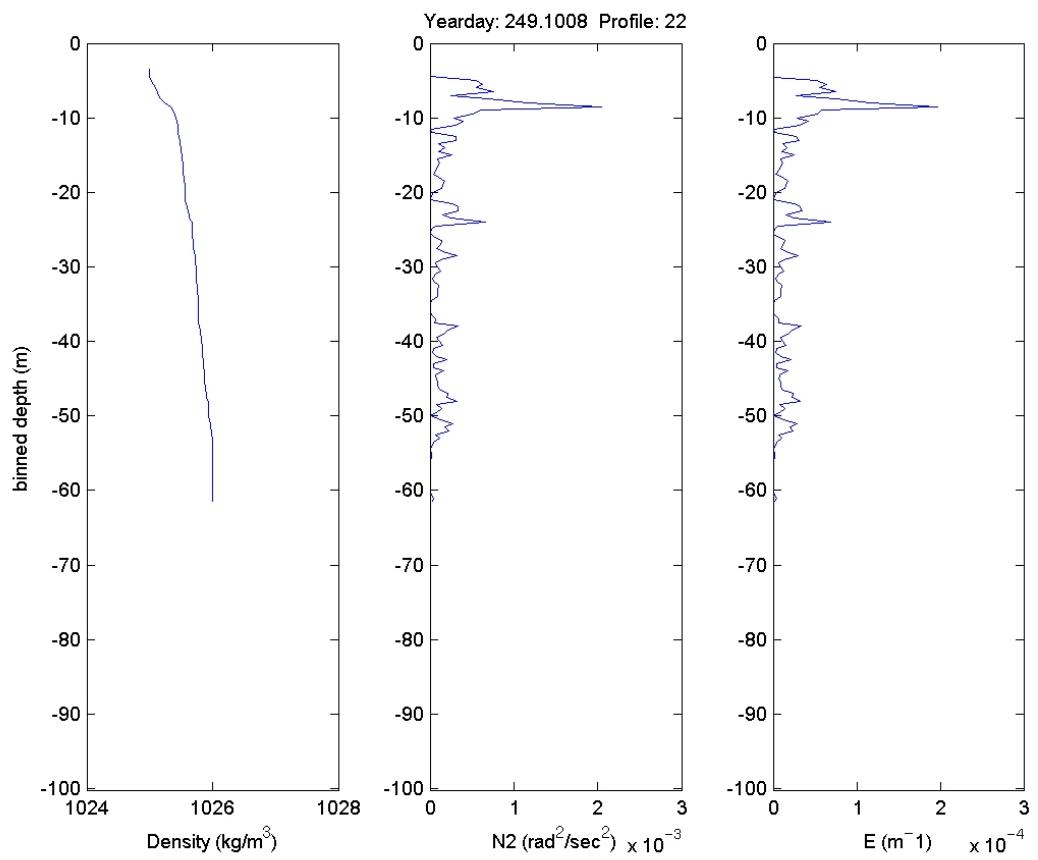
Figure 9.   YD 249.0992. Early September 2006. Profile 22, (left) Density vs. depth, (middle) N^2 vs. depth, (right) stability vs. depth.
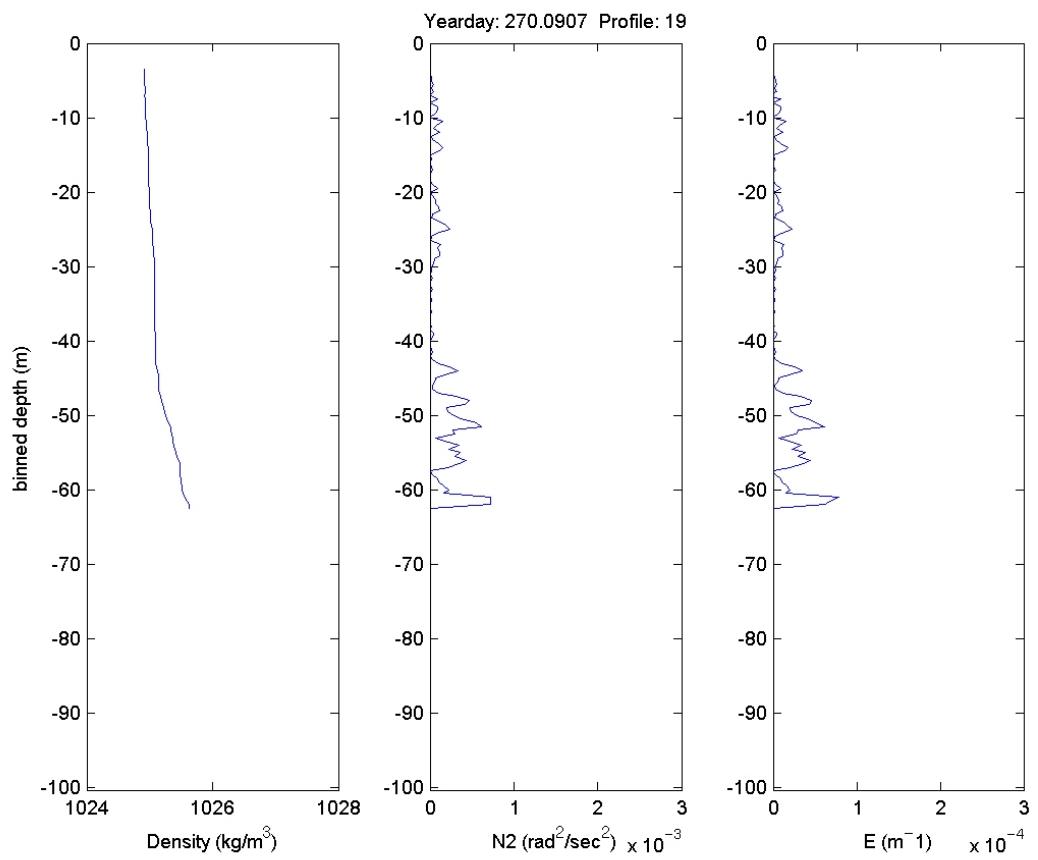
Figure 10.   YD 270.0874. Late September. Profile 19, (left) Density vs. depth, (middle) N^2 vs. depth, (right) stability vs. depth.
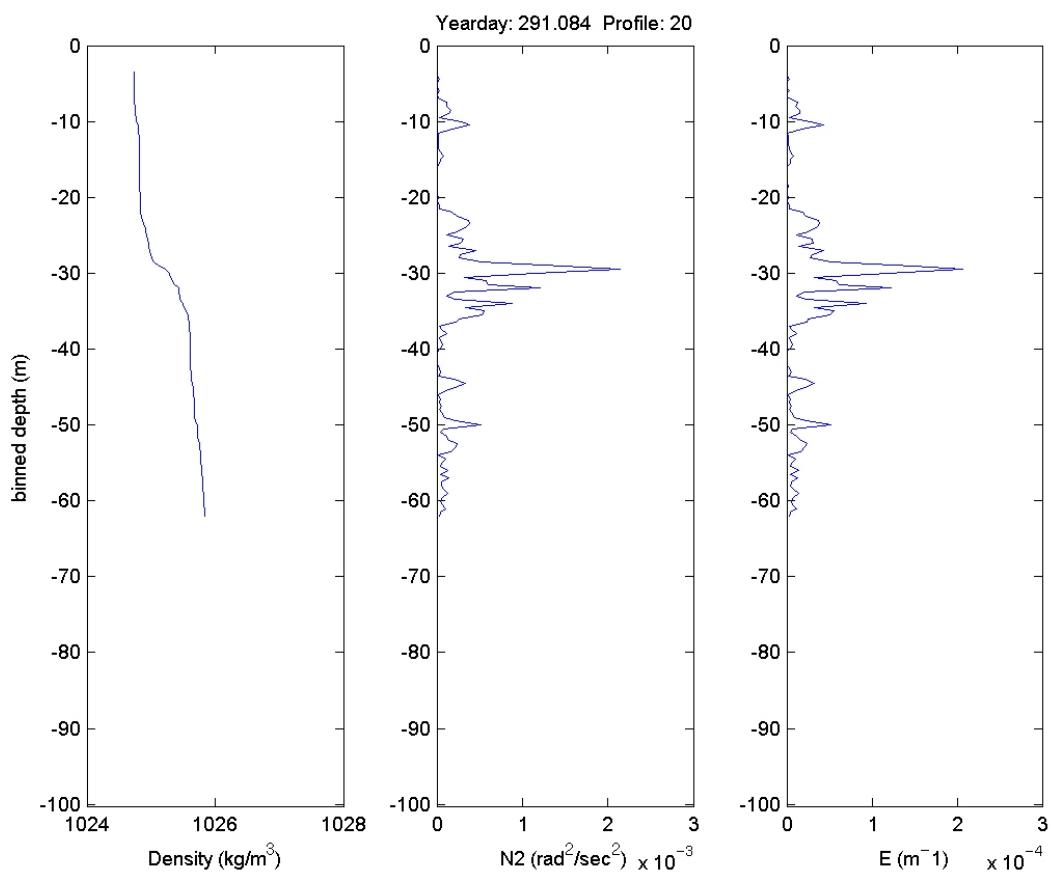
Figure 11.   YD 291.0824. October 2006. Profile 20, (left) Density vs. depth, (middle) N^2 vs. depth, (right) stability vs. depth.
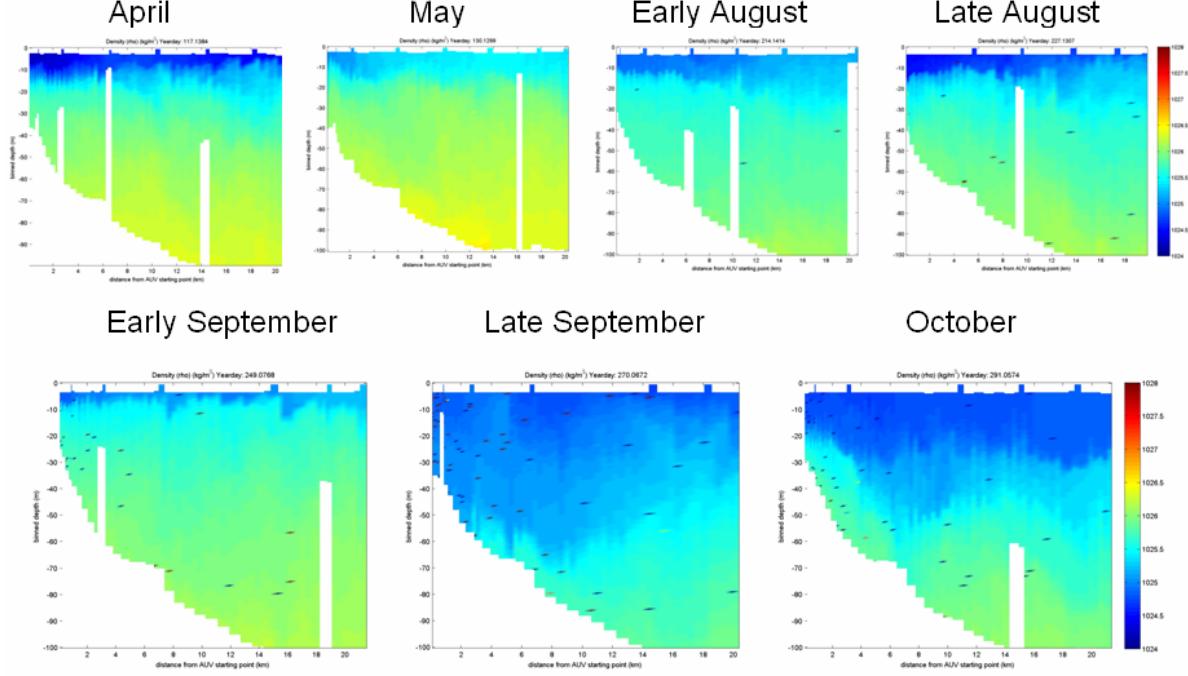
Figure 12.   Density plots: AUV data from spring through fall of 2006. April (top left), May, early August, late August, early September, late September, and October (left to right, top to bottom). Deeper blue colors represent lower density while yellow colors represent higher density. A more distinct interface between blue and yellow indicates higher stratification.

2.   Ideal Conditions: Summer

AUV data showed that near-surface shelf stratification and increased maximum buoyancy frequencies existed during the summer of 2006. Figure 13, generated from MISO data, shows the tidal amplitude and stratification conditions at MISO during the summer of 2006. Panel 1 shows the tidal signature time series measured by the paro-scientific pressure transducer. Panel 2 depicts the tidal amplitude at the time of each recorded event described in the following chapters. Panel 3 shows the maximum temperature gradient during the quiescent state estimated from the thermistor string. The "quiescent state" was determined using mean temperature values from 1 hour prior to each event. Maximum temperature gradient values were calculated for comparison to density gradient, or buoyancy frequency, maxima calculated from AUV data. Maximum temperature gradients were highest during late July, August, and early September (YD 202-262) and were remarkably constant during this time. Temperature gradient maxima

averaged 0.4 °C/m with a maximum value reaching 1.4 °C/m. Data prior to YD 202 and post YD 262 has not been shown because maximum temperature gradients were low and averaged only 0.1 °C/m. MISO and AUV data both indicate that on shelf stratification was robust in the summer of 2006. Monterey Bay's summer meteorological conditions, including low to moderate amplitude winds, a diurnal afternoon sea breeze, few storms, and local surface heating contributed to the development of this shelf stratification.
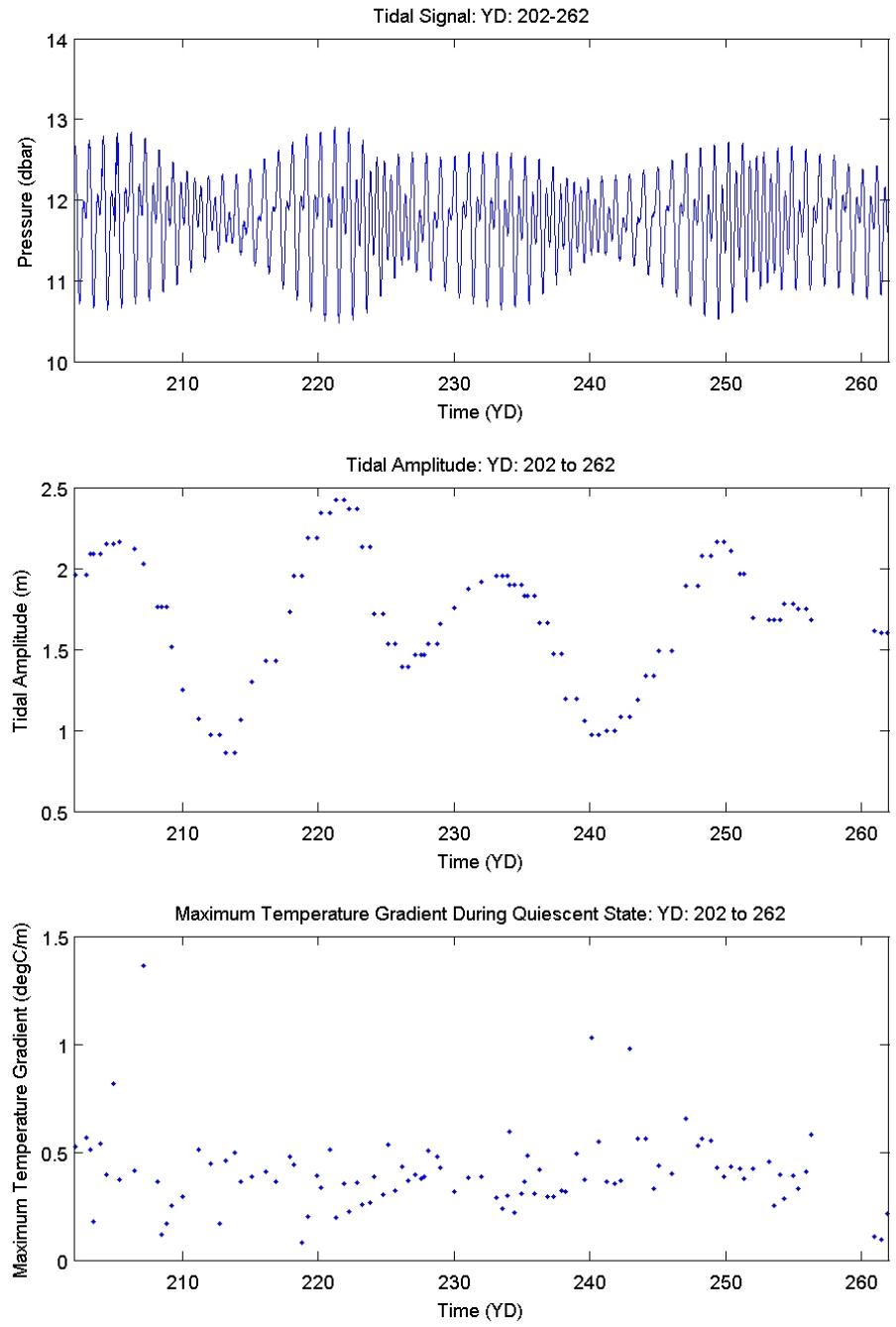
Figure 13.   Tidal signal, tidal amplitude, and maximum temperature gradient for the
          period of most significant internal tidal bore activity, YD 202-262.

THIS PAGE INTENTIONALLY LEFT BLANK

II. DATA ACQUISITION

A. THE MONTEREY INNER SHELF OBSERVATORY

Data used for this internal tidal event assessment was gathered from instruments employed in the southern portion of the Monterey Bay at the Monterey Inner Shelf Observatory (MISO). MISO is a component of the Rapid Environmental Assessment Lab (REAL) that serves oceanographers and students at the Naval Postgraduate School (NPS) in Monterey, California. MISO was designed and implemented in 2000 by Tim Stanton and the ocean turbulence research group at NPS. The site and associated research is ongoing and is supported by the NPS Oceanography department and the Office of Naval Research (Stanton 1998).

The MISO instrument frame is located 600 m out from the Del Monte beach adjacent to the Naval Postgraduate School, Figure 14. The frame is anchored in the sand and stands in approximately 12 m of water. The long-term, continuous observations from the MISO site and REAL laboratory enable studies that encompass a range of littoral oceanography observation and modeling programs.

Figure 14.   Picture identifying the MISO site in relation to the Del Monte Beach. Monterey Harbor is visible in the upper left corner of the picture. The reader may note that the MISO instrument frame is in fairly shallow water (between 10 and 15 m deep) and is nearshore. (From Stanton 1998)

B.   EQUIPMENT AND ACQUISITION METHODS

1.   Overview

Constructed of stainless steel, the MISO instrument frame suspends oceanographic instruments about 1 m above the sandy bed. Long-term observations of inner shelf processes are made possible by the rugged and durable instrument frame, high bandwidth communications, and a continuous power available with a cabled observatory. (Stanton 1998)

The MISO frame supports several long-term instruments including a high precision digital (Paro-scientific) pressure sensor and an Acoustic Doppler Current Profiler (ADCP). The continuous ADCP and pressure data combined with a 16 element, 0.5 m spaced thermistor string deployed in June of 2006 was used in this analysis.

Wind data was gathered from the REAL MET instrument tower located approximately 700 m directly shoreward of the MISO instrument frame on the sand dune above Del Monte Beach.

2. Acoustic Doppler Current Profiler (ADCP)

Vertical current profiles are made with an upward looking Workhorse Monitor Acoustic Doppler Current Profiler (ADCP) mounted on the MISO instrument frame. The ADCP (RD Instruments) sends "pings" through the water column by transmitting a broadband acoustic pulse along 4 narrow convex acoustic beams each angled 20° from the vertical (Marine Measurements 2007). The 4-beam design and an independent measurement known as error velocity provide redundancy and quality in data gathering (Marine Measurements 2007). Each of the four transducers uses Doppler shifts from scatterers to determine water column velocities. Combining ping results, the four measured Doppler shifts at each range bin can be resolved into u, v, and w velocity components. At the MISO site, the ADCP (Figure 15) measures current vectors in the cross-shore and along-shore directions every 0.5 m over 24 equally spaced bins from 0.8 m beyond its location to near the surface. The bins nearest the surface are often contaminated due to surface reflection, and are, therefore, not reliable.

Figure 15.   Workhorse Monitor Acoustic Doppler Current Profiler (ADCP) mounted on the MISO instrument frame. Manufactured by RD Instruments. (From Stanton 1998)

C. DATA LOGGING

Data was gathered at different sampling intervals; therefore, all of the data had to be coupled to one time axis to plot and combine results. Temperature, current velocity, wind speed, and backscatter data were all gathered at different time increments. A turbulence group MATLAB program called RESECT was applied to resample or interpolate data as needed to create a prescribed 30 second sampled time axis.

The 2006 data used in this assessment spanned YD 182 to 362. Within that time, there were some gaps in data where equipment readings were not available. This occurred very infrequently. Of the 180 days being assessed, approximately 7 days worth of data were unusable.

III. DATA PROCESSING AND ANALYSIS

A. ANALYSIS TECHNIQUES AND METHODS

1. Coordinate Transformation

To facilitate field data analysis, ADCP current profile and wind data were rotated to a cross-shore (CS) normal coordinate system with a +x axis along the Monterey Bay coast towards Marina and +y axis depicting the offshore direction. Figure 16 provides a graphical representation of the coordinate system. Height above bed, was chosen for the vertical axis, with +z upwards.
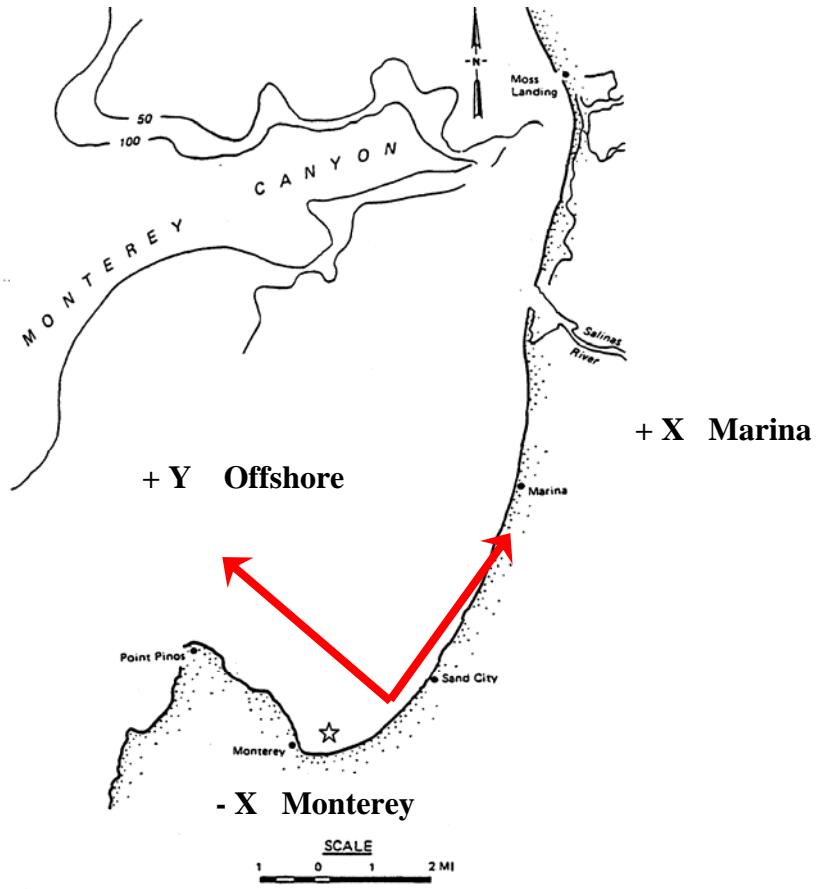
Figure 16.   Map depicting coordinate system. The Y-direction is associated with the cross-shore direction while the X-direction is the along-shore direction. The star marks MISO. (From Tjoa 2003)

ADCP data is collected in a +/- **u** (East/West) and +/- **v** (North/South) coordinate system with respect to earth's magnetic north. Shore normal to the beach was measured to be 320° magnetic. A -40° transformation allows data to be described as "along-shore" (the X direction) or "cross-shore" (the Y direction).

To observe the effects of wind forcing, wind data were coupled to ADCP data and rotated to the same cross-shore normal coordinate system. Wind measurements were made in a true coordinate system. Wind speed and direction were used to compute the **u** and **v** wind components. The **u** and **v** components were then transformed into the CS normal coordinate system with onshore winds described as negative and winds blowing from Monterey towards Marina described as positive.

2. Isotherms

Temperature profile time series were used to identify internal bore and soliton activity in Monterey's inner shelf water column. Because large amplitude vertical displacements of isotherms define bore and soliton events, plunging isotherms were used to identify the leading edges of internal tidal bore (ITB) events and the solitons associated with them. Using graphical user input and visual analysis, bore events were identified and the time of the center of the leading edge of each bore event was recorded. Temperature, current, wind, pressure, and backscatter data from each "event time" was then extracted in order to characterize them. In order to correctly estimate conditions at the ITB event's leading edge, an isotherm-tracking sampling scheme was used to sample currents over an hour long averaging period. The isotherm-tracking sampling scheme ensured that sampling occurred within the upper layer of the bore.

The leading edge of the bore or solibore packet was used to determine the "event time" because the leading edge of an ITB has the strongest current signature. Figure 17 depicts the temperature profile and associated isotherms for YD 242–246. Seven internal tidal events were marked. The time of each mark was recorded. The events varied in duration and occurred at different time intervals; however, each event was identified by its leading edge.
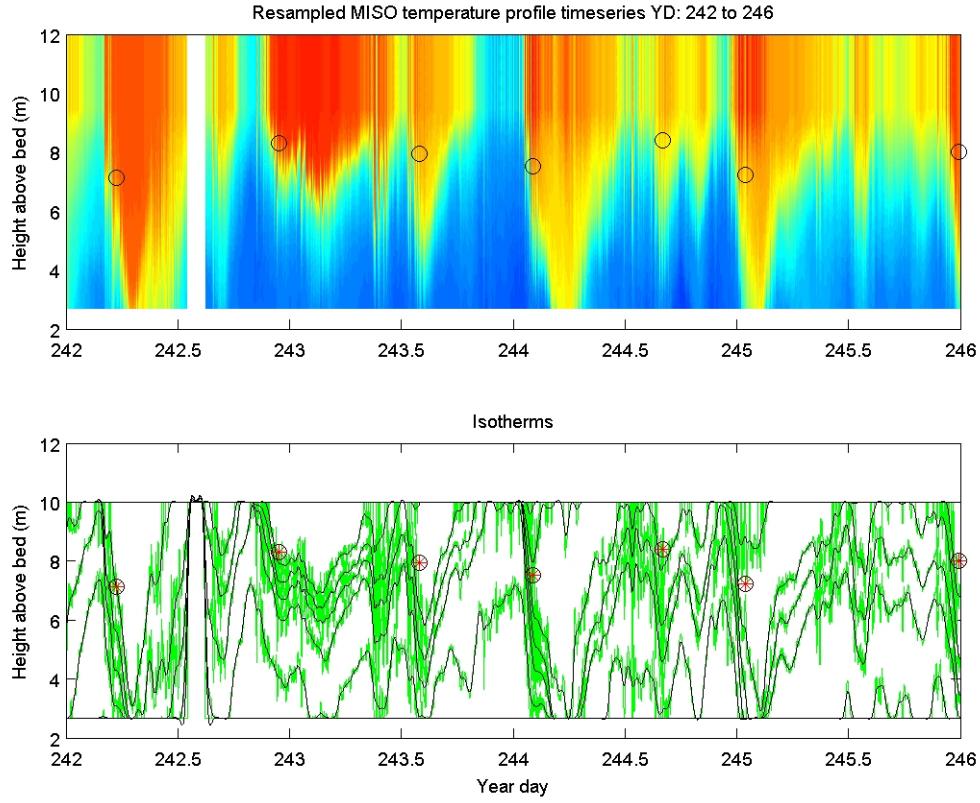
Figure 17.   Graphic depicting temperature signature and isotherm signature of events in upper and lower panels, respectively. Data from YD 242-246 is shown. Isotherms were used to identify bores and solitons. In the upper panel, open black circles indicate the points chosen to identify event times. In the lower panel, red asterisks mark event times.

3.   Current Vector Plots

After event times were collected using the isotherm and leading edge method, current velocity data specific to the event was extracted from the entire MISO data set. Current data from MISO was organized into 24 depth bins beginning with bin 1 nearest the bed and bin 24 farthest from the bed. The isotherm-tracking sampling technique was used to characterize upper column current velocities while data from bins 3-5 were used to determine lower column current velocities. Upper and lower column current velocities were plotted to compare ITB event current characteristics. Current data from the leading edge of each ITB event were plotted as cross-shore (CS) velocity versus along-shore

29

(AS) velocity. Upper and lower column current characteristics during a bore event were graphed separately. These plots indicated whether CS or AS currents were dominant and noted any differences between the upper and lower column current magnitudes or directions during the bore event. Figure 18 is an example of a current vector plot. Each bore event was assigned a unique number which tagged the mean velocity vector for each event.
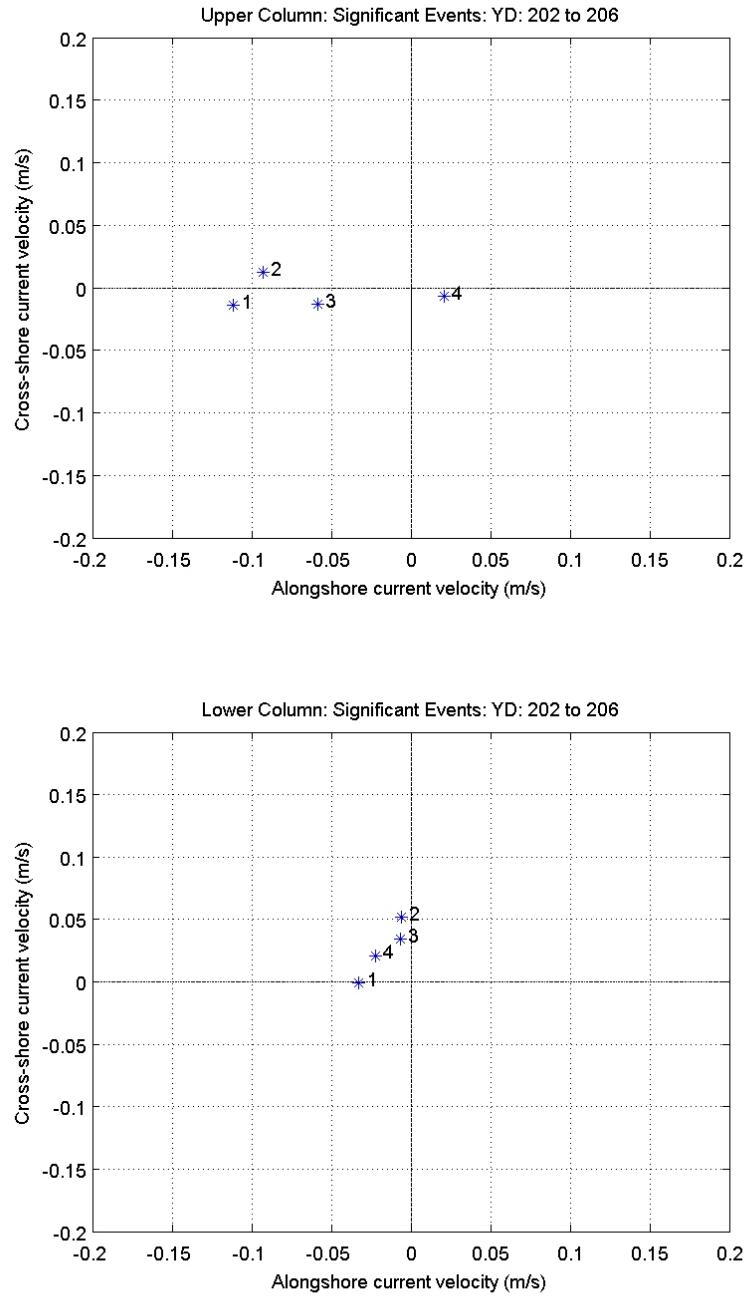
Figure 18.   YD 202-206 Current vector plot of significant events. Significant events include internal tidal bores, solibores, and solitons. The upper panel shows upper column leading edge current velocity samplings per significant event. The lower panel shows lower column leading edge current velocity samplings per significant event. Asterisk 1 identifies the first event to occur and asterisk 4 identifies the last event in the series.

31

4.   Statistical Analysis

In addition to visual analysis of isotherms and current vector plots, linear regressions and histograms were completed on all or select parts of the data to formally describe the statistical dependence of variables on one another. First order least squares regressions were performed and plotted using a turbulence group MATLAB function titled REGRES. The function generated the correlation coefficient (R). When the absolute value of 'R' is near 1, then the two variables being tested are deemed dependent on one another. When 'R' is near zero, the variables are considered to be independent. The regressions were useful for assessing the impact of winds, currents, and tidal amplitudes on ITB events. Furthermore, the correlation coefficient enabled the comparisons of ITB dependencies on very different forcing factors. One complication involved with this analysis was that the number of analyzed events varied for each 'R' calculation. The differing number of events translated to varying degrees of freedom per 'R' calculation. Histograms were used to describe the relationship between ebb tidal amplitude and event occurrence.

IV. OBSERVATIONS

A. INDIVIDUAL INTERNAL TIDAL BORE EVENTS

Observations are analyzed over a 6 month period during the late summer of 2006, spanning YD 182 through YD 362 (early July through late December). Internal tidal bores (ITB events) were observed throughout the entire data set; however, distinct and consistent ITB activity occurred from YD 202 through YD 262 (late July through mid-September). This study focuses on that period of distinct activity that occurred YD 202-262 because ITB events were infrequent at other times. Additionally, this period of high ITB activity occurred during the time that AUV and MISO data indicated the strongest near surface stratification in Monterey Bay.

For this discussion, ITB events were classified into three subgroups: bore events, bore events with solitons (solibores), or soliton events; however, the term ITB is used to refer to all three types of events. ITB events have many characteristics that may differentiate one event from another and provide evidence of their origin. During the observation period, ITB events were observed to have both significant cross-shore (CS) and along-shore (AS) velocity signatures. In some cases, the CS velocity signature was more dominant; in others, the AS velocity signature was more dominant. Additionally, at the shallow and strongly shoaled MISO site, the current structure was not always resolved in the vertical since the ITB events often occupied the water column to the depth of the deepest thermistor and ADCP bin. Four time periods, each with a highlighted event, have been chosen to illustrate the differences between ITB events.

1. YD 208-208.5 Internal Tidal Bore Event

Figure 19 spans YD 206-210 and is a period characterized by narrow steep bores of varying depth excursion and few solitons. Panel 1 of Figure 19 represents the temperature profile time series. CS and AS velocity profile time series are shown in panels 2 and 3. Current reversals (vertical shear) associated with bores can be most clearly seen in the pycnocline (represented by the yellow colors in the plot). Blue cross-shore velocities represent onshore flow, and red offshore, with blue along-shore velocities indicating motion towards Monterey. The plot in panel 4 of Figure 19 displays

the water column depth, or tidal signature, showing where events occurred with respect to tidal ebbs and floods. Finally, panel 5 displays the wind time series which indicates winds were predominantly onshore and towards Monterey.

The ITB event that occurred during YD 208-208.5 was chosen to represent the group of events highlighted in Figure 19. The thermal signature of the YD 208-208.5 event is shown in panel 1 of Figure 20. The bore event has leading edge solitons seen as deep red temperature excursions in panel 1 of Figure 20; therefore, it can be termed a solibore event or an ITB with solitons. The duration of the event extended from YD 208.13 to 208.32, corresponding to approximately .19 YD or 4.6 hours. Three solitons were identified on the solibore's leading edge. These solitons were low amplitude and not as easily distinguished as were other solitons observed at MISO. The ITB event's amplitude was ~ 5 m. The temperature differential of the bore and the background temperature was greatest at the solibore's leading edge with a maximum differential of approximately 3-4°C. The thermocline location prior to the arrival of the ITB was approximately > 9 m above the bed, above the highest thermistor.

Prior to the ITB event's arrival at MISO, upper column cross-shore currents were weakly positive, or offshore, while along-shore currents were weakly negative, or towards Monterey Harbor. Lower column cross-shore and along-shore currents were near zero. During the ITB event, the cross-shore current signature revealed a negative or onshore pulse in the upper column while lower column currents shifted towards the positive, or offshore, direction. The along-shore currents during the bore event also display a strongly negative pulse towards Monterey. After the bore passed the MISO site, upper level cross-shore currents returned to the conditions observed prior to the ITB event's passage. Lower column cross-shore currents reversed to be strongly onshore. Upper and lower column along-shore currents tended to be more positive, or towards Marina, following the ITB. The strong upper column onshore motion and lower column offshore motion of the cross-shore currents during the event indicate a significant non-linear cross-shore transport with an upper level shoreward mass flux and a corresponding offshore flow felt near the bed. The third panel of Figure 20 shows the backscatter signature during the event. An increase in backscatter was observed along the interface of the ITB and the lower layer of water. The increase in backscatter and the presence of

current fluctuations at the same location in the water column verifies isotherm data as representative of the ITB event's primary density interface location. Ellipses in Figure 20 highlight a portion of this location. The strong current shear confined to the interface indicates mode 1 characteristics.
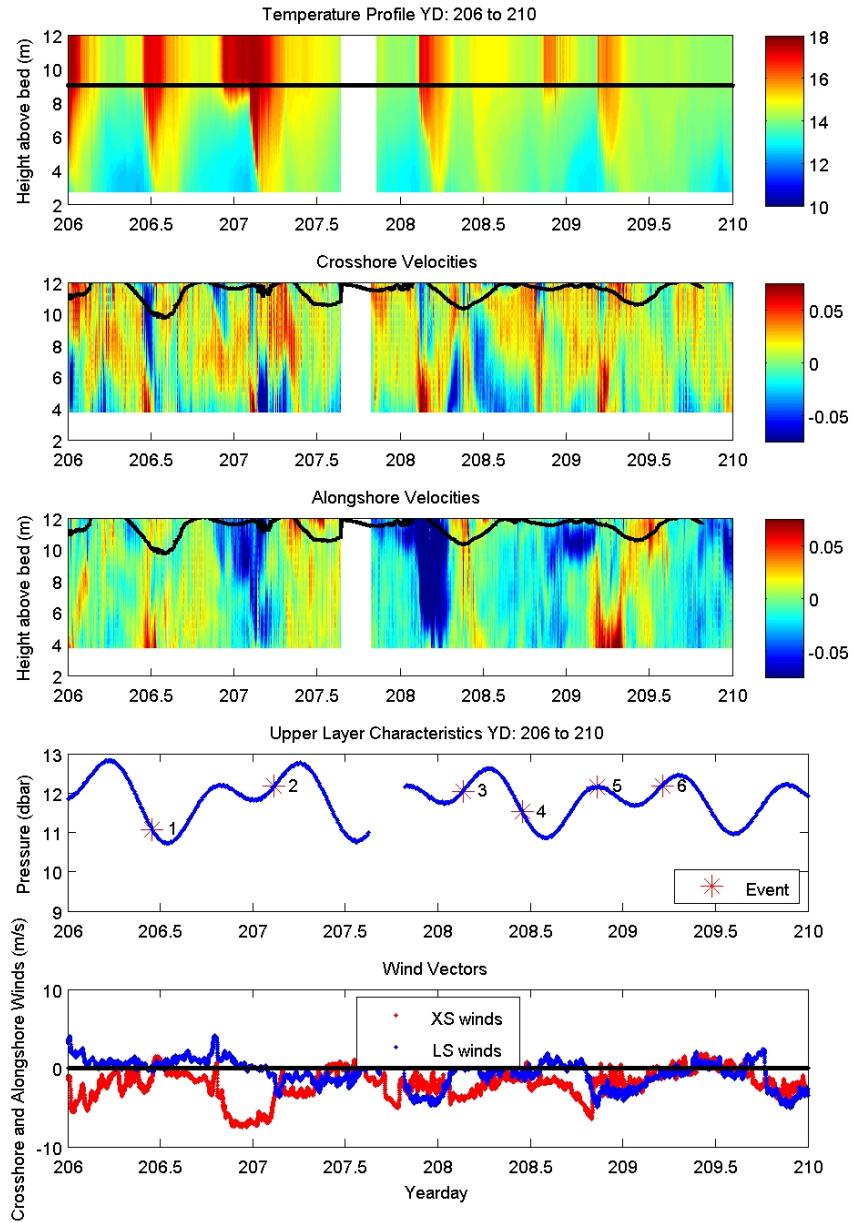
Figure 19.   YD 206-210. Temperature signature shown in panel 1. The black line indicates the depth of the highest thermistor. Temperature data above the line is interpolated. Cross-shore and along-shore current velocities are depicted in panels 2 and 3, respectively. The black lines in panels 2 and 3 represent surface height. Data above the surface height is interpolated. Tidal signature with asterisks marking event times shown in 4th panel. Cross-shore and along-shore winds depicted in last panel. Negative cross-shore quantities indicate onshore motion. Negative along-shore quantities indicate motion towards Monterey.
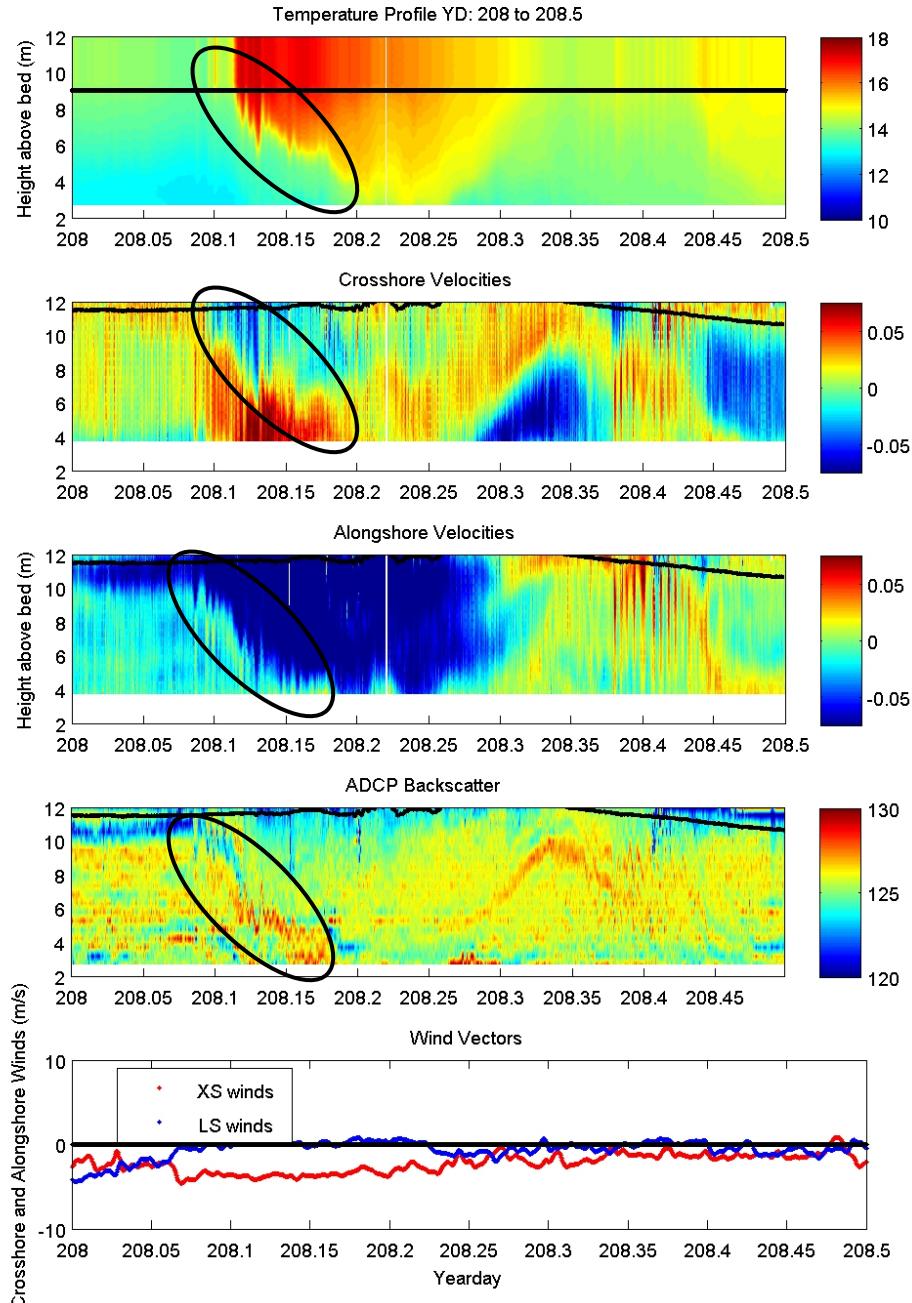
Figure 20.   Solibore event: YD 208-208.5. Top panel represents temperature characteristics in degrees Celsius, panel 2 indicates cross-shore current velocity in m/s, panel 3 depicts along-shore current velocity in m/s, and the last panel displays cross-shore and along-shore winds in m/s. Ellipses highlight a portion of the density interface location which is confirmed in temperature, current, and backscatter data.

## 2.	YD 229-229.25 Internal Tidal Bore Event

The ITB events associated with YD 226-230 occur at high frequencies and have durations similar to the event of YD 208-208.5. The events of this four day time period have depth excursions that exceed the deepest thermistor. Temperature signatures of the events can be seen in the top panel of Figure 21. The events of YD 226-230 are nearly uniform in shape and occur at more regular intervals of time than the events of YD 206-210. The event of YD 229-229.25 was expanded to represent the aforementioned group of events. Figure 22 shows the structure of this highlighted ITB. Two significant solitons are present at the leading edge of the ITB. Its duration is approximately .2 of a year day, or 4.8 hours. The thermocline location prior to the ITB was 5-7 m above the bed which is slightly lower in the water column than the event of YD 208-208.5. The ITB event's maximum depth excursion exceeds the depth of the deepest thermistor. The depth of the thermocline and the mode 1 characteristics of ITB events may contribute to the maximum depth excursion of this ITB reaching the deepest thermistor. The maximum temperature differential associated with the bore is 4-5°C and is located at the event's leading edge.

In both the cross-shore and along-shore directions, a negative pulse is associated with the passage of the ITB's leading edge. The current reversal throughout the water column is most distinct in the cross-shore direction, however, where both upper and lower column currents completely reverse. During the ITB, upper column cross-shore currents are strongly onshore while lower column cross-shore current is offshore. Along-shore currents in the upper column display a much weaker signal and remain predominantly positive, or towards Marina, prior to and during the ITB event. In the middle of the water column, along-shore currents are negative, or towards Monterey. The backscatter plot in panel 4 of Figure 22 depicts a density increase in scatterers along the event's edge. Winds during the event were consistently onshore and towards Monterey.
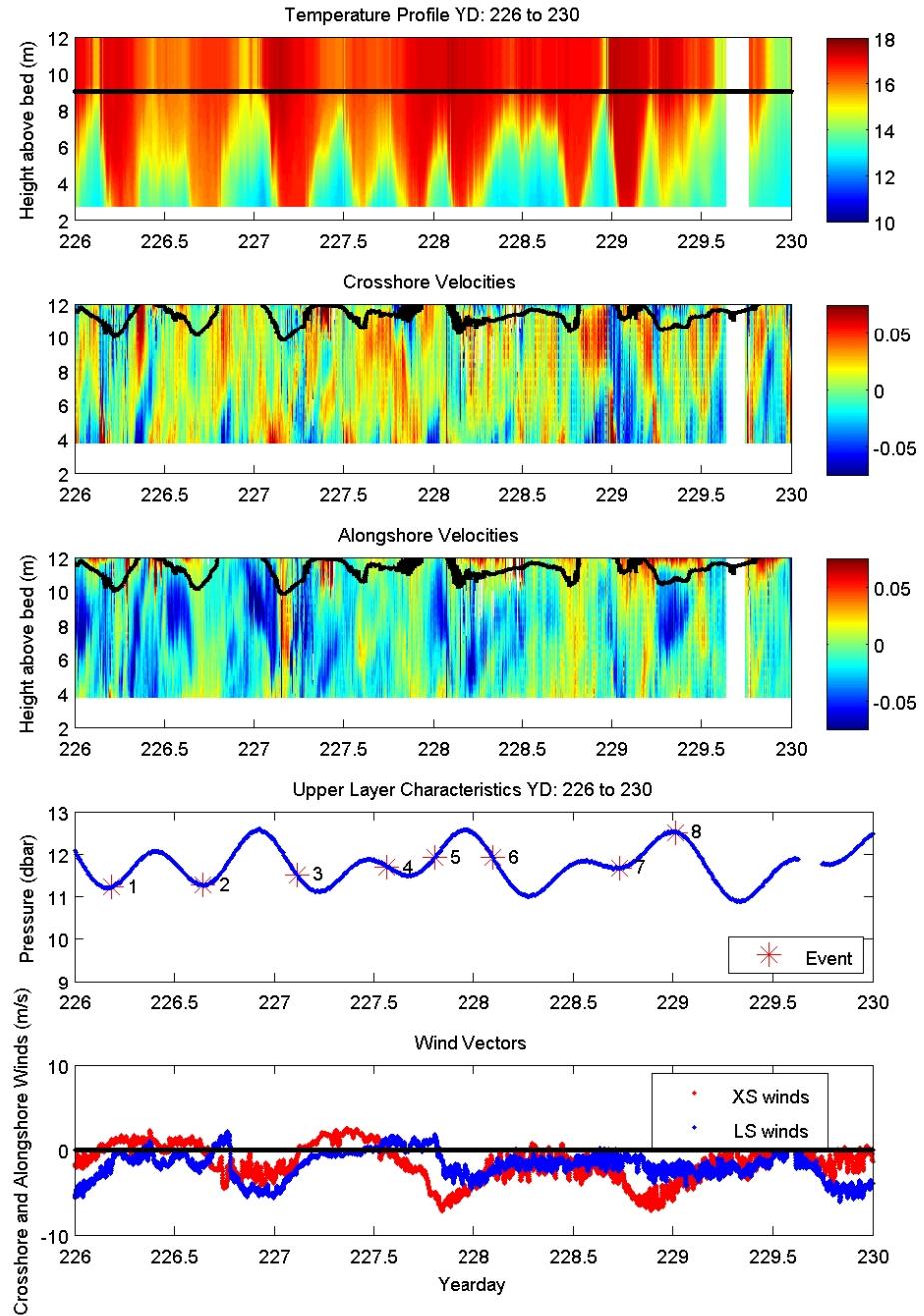
Figure 21.   YD 226-230. Temperature signature in panel 1. Cross-shore and along-shore current velocities depicted in panels 2 and 3, respectively. Tidal signature with asterisks marking event times in 4th panel. Cross-shore and along-shore winds depicted in last panel.
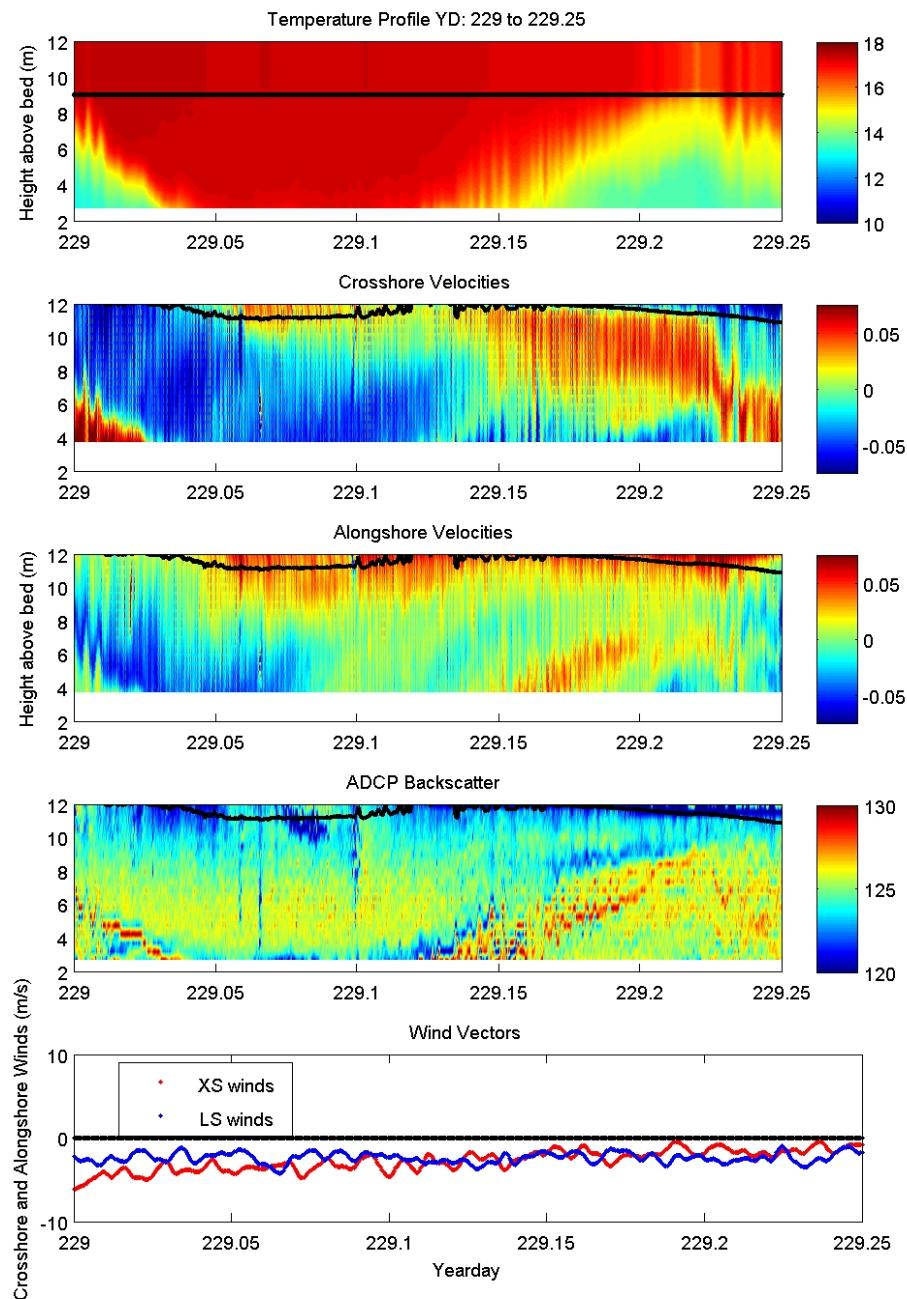
Figure 22.   Internal tidal bore (ITB) event: YD 229-229.25. Top panel represents temperature characteristics of water column in degrees Celsius, panel 2 indicates cross-shore current velocity in m/s, panel 3 depicts along-shore current velocity in m/s, and the last panel displays cross-shore and along-shore winds in m/s.

3.   YD 244-244.5 Internal Tidal Bore Event

The ITB event that occurred during YD 244-244.5 was chosen to represent the conditions present during YD 242-246. The thermal structures of the YD 242-246 ITB events can be seen in Figure 23. The events are highly variable in form. These ITB events occur at widely varying intervals and isotherm excursion depths in comparison to other four day increments of data. The ITB event of YD 244-244.5 is depicted in Figure 24 and was longer in duration than the events observed in YD 208-208.5 and YD 229-229.25. The bore and its associated rank ordered solitons span YD 244.05-244.45, or .4 of a year day, which corresponds to approximately 9.6 hours. The 12 distinct solitons along the leading edge of this event are of greater quantity than those in the YD 208-208.5 example. The greatest temperature differentials are again seen at the solibore's leading edge where at least 12 solitons were distinguished. The temperature gradient along the ITB's edge reached 5°C while the bore stratification was more spread in depth after the leading edge. The thermocline was determined to be above the highest thermistor.

Significant current changes occurred during the ITB cycle. Prior to the ITB event, both upper and lower column cross-shore current velocities were weakly positive, or offshore. The upper column along-shore current velocity was negative towards Monterey while the lower column along-shore currents were near zero. During the ITB event, strong mode 1 motions cause the upper column cross-shore currents reverse to the onshore direction while lower column cross-shore velocities become more strongly positive, or offshore. Upper and lower column along-shore current velocities maintained their negative and positive directions, respectively; however, lower column along-shore current velocities became more strongly positive, or away from Monterey.

The strongest current signatures were located at the leading edge of the solibore. Note that the first half of the event has velocity levels that are greater in both the cross-shore and along-shore directions than the color range selected. The presence of solitons indicates that the event was strong and very nonlinear, with energy transferring into higher frequency solitons on the steep leading edge. The backscatter plot confirms that

the ITB surface layer supported an increased number of scatters and that the primary density interface of the water column tracked the isotherms. Winds were consistently small.

The ITB of YD 244-244.5 is especially significant because of the many distinct solitons on its leading edge. These solitons made the temperature and current differential signatures much more distinct; however, they posed a large challenge to accurate current sampling and emphasized the need for isotherm-tracked sampling.
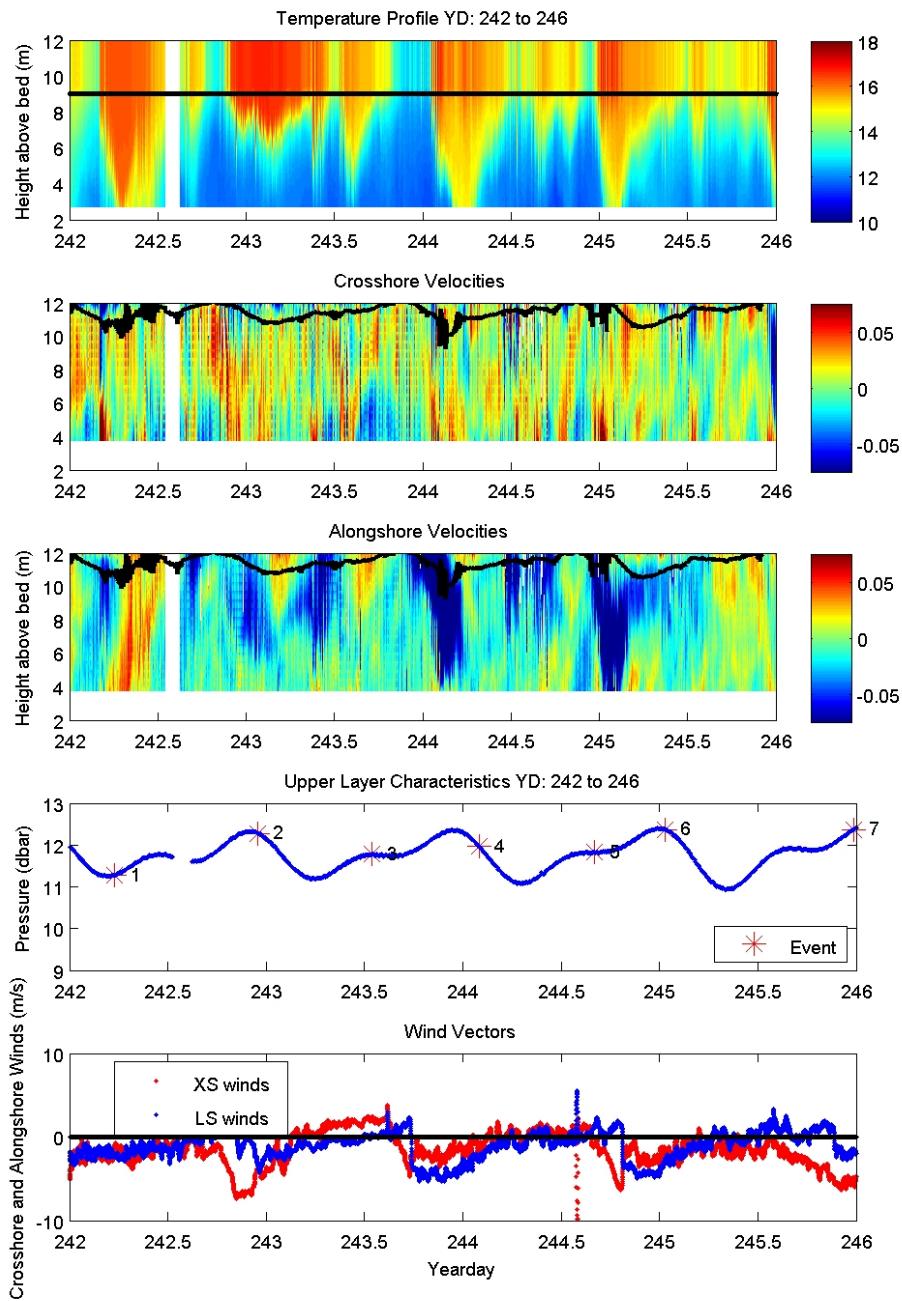
Figure 23.   YD 242-246. Temperatures and current velocities depicted in upper three panels. Tidal signature with asterisks marking event times in 4th panel. Cross-shore and along-shore winds depicted in last panel.
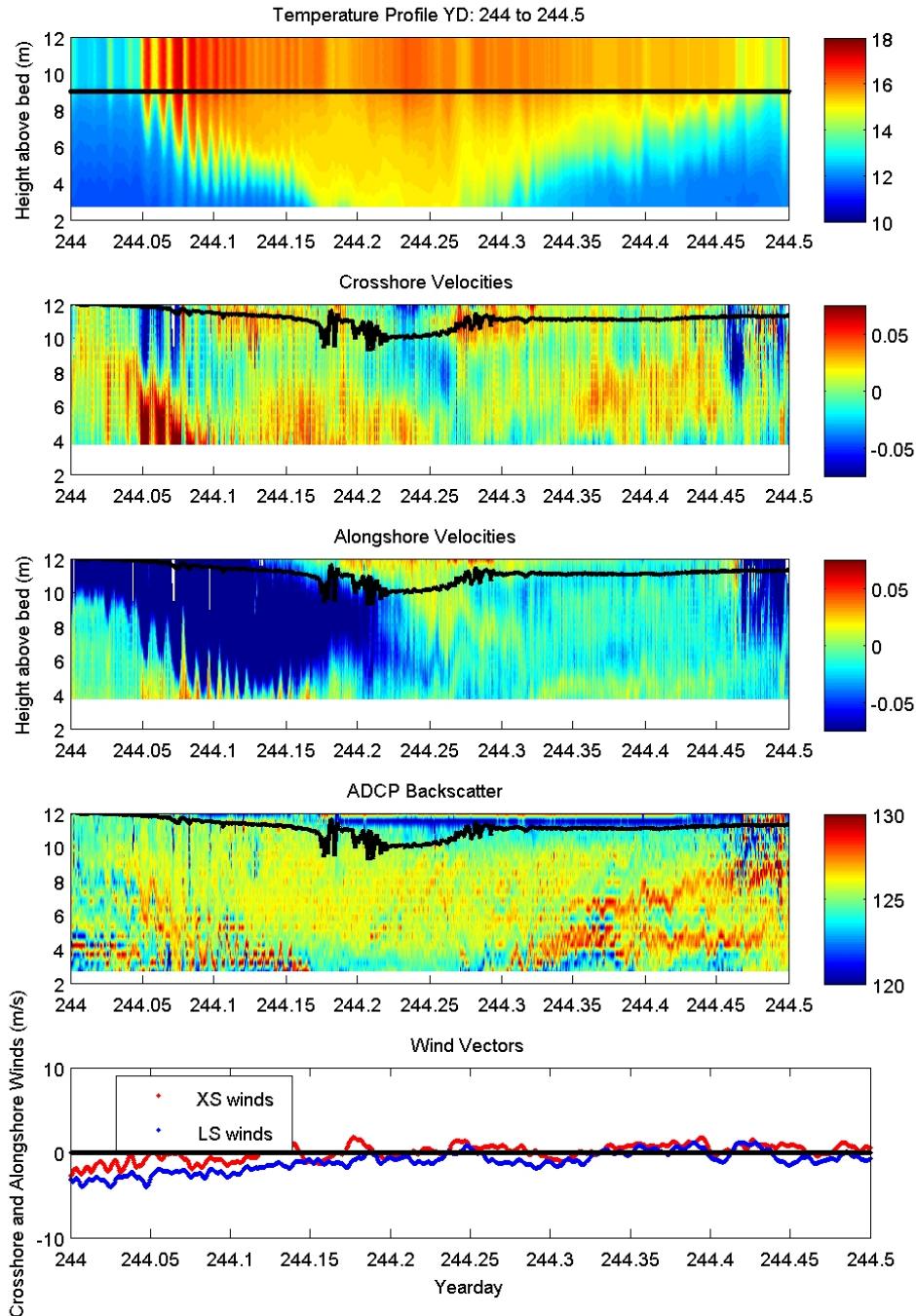
Figure 24.   Internal tidal bore (ITB) event: YD 244-244.5. Top panel represents
     temperature characteristics of water column in degrees Celsius, panel 2 indicates
   cross-shore current velocity in m/s, panel 3 depicts along-shore current velocity in
     m/s, and the last panel displays cross-shore and along-shore winds in m/s.

4. YD 247-247.5 Internal Tidal Bore Event

The ITB event of YD 247-247.5 was shorter in duration and smaller in amplitude than the other highlighted events with a maximum depth excursion that reached approximately 3 m above the bed. Several small (1-2 m in depth) solitons were associated with the event just prior to the leading edge of the bore. This event represents the narrow deep irregular bores with associated solitons seen in Figure 25, YD 246-250. The duration of the highlighted YD 247-247.5 event, Figure 26, extended from approximately 247.02-247.24 corresponding to .22 of a year day, or 5.3 hours. The maximum vertical temperature differential across the upper and lower layer was again associated with the ITB's leading edge and was 4°C. Prior to the ITB event, the thermocline was ~8 m above the bed.

A significant feature of this bore is the strong onshore pulse associated with the bore. Prior to the ITB's arrival, cross-shore velocities throughout the water column were weakly positive (offshore) while upper level along-shore velocities were weakly negative (towards Monterey) and lower level along-shore current velocities were near zero. Cross-shore currents demonstrated the strongest variability during the ITB event. A strong upper column onshore pulse and lower column offshore pulse was associated with the ITB's passage. Change in the along-shore direction was weak. The backscatter plot in panel 3 of Figure 26 indicates an increased number of scatterers at the ITB's leading edge. One predominant soliton can be seen in the current and backscatter signatures. Winds were consistently onshore and towards Monterey and had small magnitude.
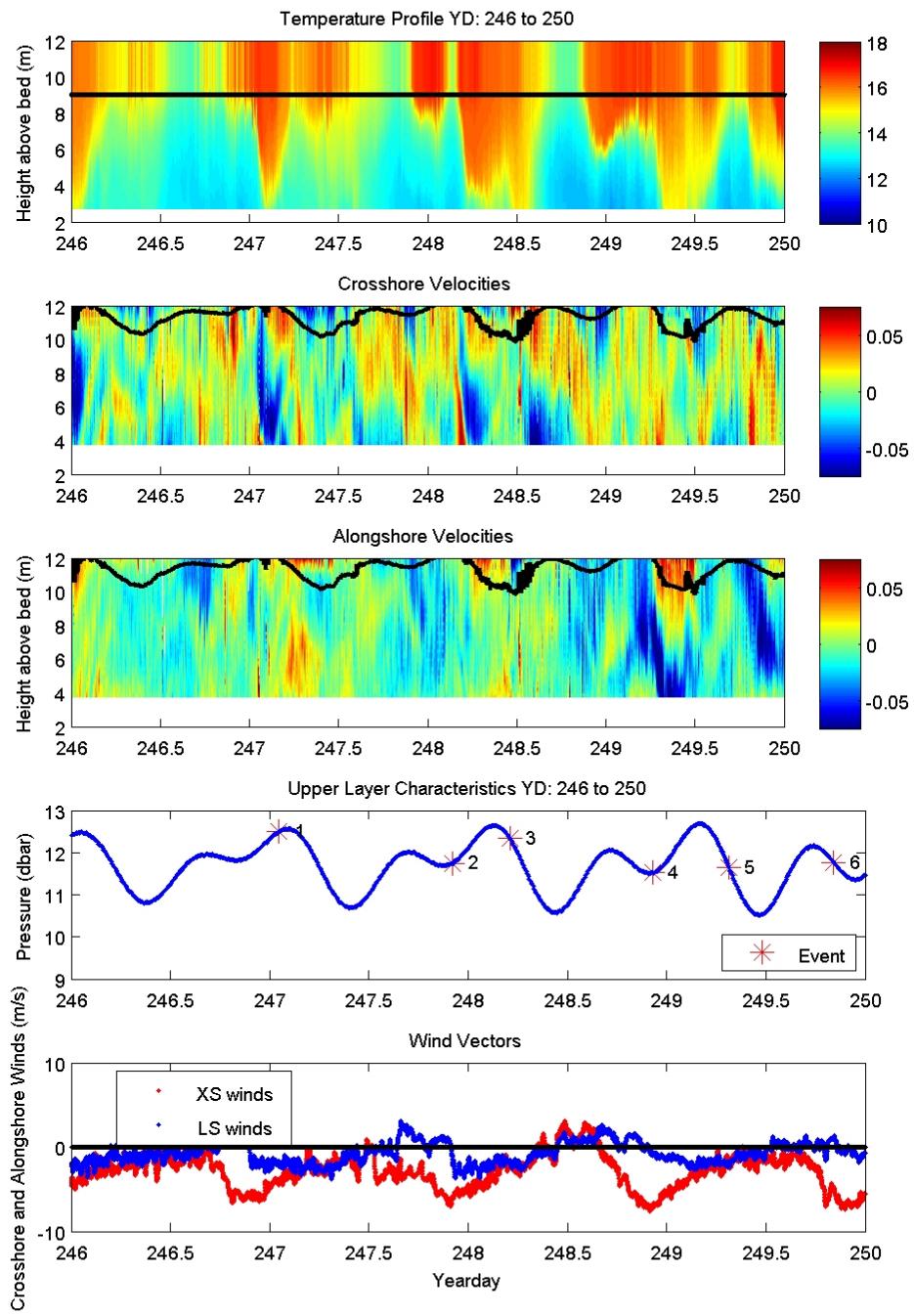
Figure 25.   YD 246-250. Temperature signature in top panel. Cross-shore and along-shore current velocities depicted in panels 2 and 3, respectively. Tidal signature with asterisks marking event times in 4th panel. Cross-shore and along-shore winds depicted in last panel.
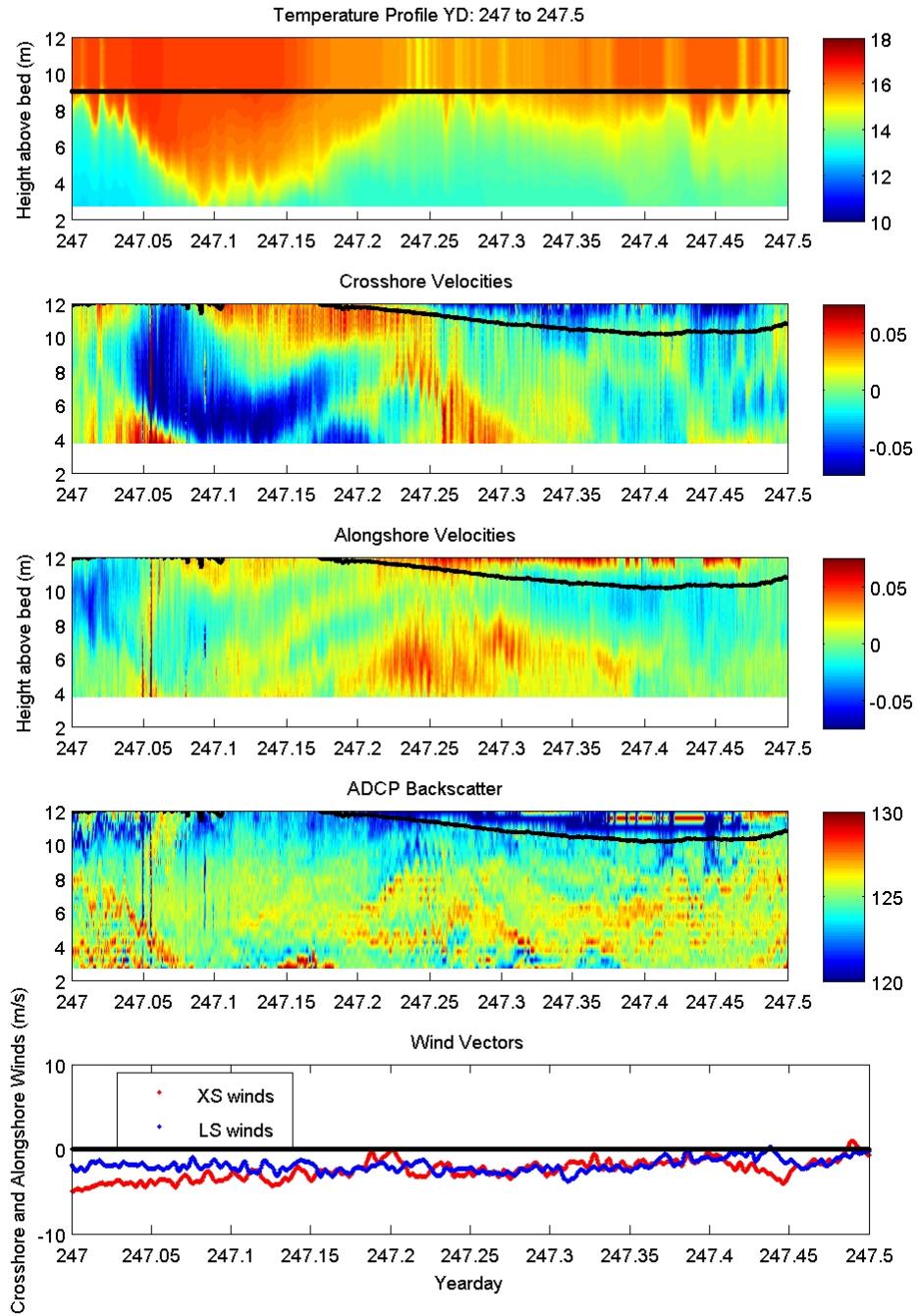
Figure 26.   Internal tidal bore (ITB) event: YD 247-247.5. Top panel represents temperature characteristics of water column in degrees Celsius, panel 2 indicates cross-shore current velocity in m/s, panel 3 depicts along-shore current velocity in m/s, panel 4 shows the backscatter characteristics of the event, and the last panel displays cross-shore and along-shore winds in m/s.

47

5.   Summary of Individual Event Characteristics

Table 2 is a summary of individual event characteristics for each of the events highlighted above in this section. Most of the events had steep leading edges and temperature differentials near 4°C. The events with fewer solitons had shorter durations than those events with more solitons. All of the backscatter plots showed increased scatterers along the upper layer edge of the ITBs. This layer of increased scatter levels tracked the isotherm displacements. The event of YD 229-229.25 had the thermocline nearest the bed. The events of YD 229-229.25 and YD 244-244.5 were the only events of the four where the upper layer occupied the whole water column. All of the events had maximum depth excursions exceeding one half of the water depth or more. The long duration of the event of YD 244-244.5 is not well understood, but the majority of events ranged 4-6 hours in duration. In most of the events, a significant onshore pulse was seen in the upper column current signature while lower column currents were characterized by net offshore motion during the leading edge. Along-shore current signatures varied in strength, but fluctuations were significant (> 5 cm/s) along the leading edges of the first 3 highlighted events. In each of these events, a strong initial negative along-shore velocity towards Monterey was observed.

ITB Event of YD:	Basic Description:	Duration: (hrs)	Vertical Temperature Differential of upper and lower layers: (°C)	Thermocline Depth Prior to ITB: (m above bed)	Current Signature Dominance:
208-208.5 (late JUL)	- narrow/steep edge - few solitons	4.6	3-4	> 9	Stronger CS Strong AS
229-229.25 (mid AUG)	-narrow/steep edge -few solitons -highly shoaled	4.8	4-5	5-7	Stronger CS Weak AS
244-244.5 (early SEPT)	-broad, more gradual edge -less shoaled -many solitons	9.6	5	> 9	Very strong CS Very strong AS
247-247.5 (early SEPT)	-narrow/steep edge -least shoaled -many solitons	5.3	4	7-9	Stronger CS Weak AS

Table 2.   Summary of highlighted ITB events and their characteristics. Duration indicates length of time that the ITB persisted. Temperature differential indicates the maximum vertical temperature gradient that occurs between the ITB's leading edge and the background waters. Note that thermocline depth indicates the thermocline location prior to the ITB and is referred to from the bed.

B.   HYPOTHESES SUMMARY

Based on initial visual observation and background knowledge of internal tides, several hypotheses were formed. First, it was hypothesized that if barotropic tidal amplitude (strength) was the dominant event forcing mechanism, then larger tidal amplitudes would be associated with stronger leading-edge event current magnitudes; particularly in the cross-shore direction. Second, due to strong diurnal afternoon sea breezes in the Monterey Bay, it was hypothesized that a positive correlation would exist between wind and current velocities, and that the wind/current correlation would be weaker than the correlation of tidal amplitude and event-associated current velocities.

The weakness of this correlation was hypothesized because the tide is thought to be the dominant forcing mechanism of ITBs during the leading edge sampling times. Third, it was hypothesized that if ITB events were generated by the lee wave mechanism, then events would be regularly observed at MISO at fairly uniform delays in relation to the occurrence of the ebb tide. Additionally, it was expected that these relationships would be more obvious if events were sorted into bore, soliton, and solibore groups through visual inspection.

The last set of hypotheses regarded current directionality and generation mechanisms. ITB events are strong shoreward pulses of warm upper layer water; therefore, it was hypothesized that upper level cross-shore leading-edge currents would indicate net onshore motion and lower column leading-edge currents would indicate net offshore motion in conjunction with a lower layer return flow.

It was also hypothesized that if upper level along-shore leading-edge current signatures were predominantly negative (towards Monterey), then ITB events were most likely generated in one of two ways. First, the ITBs could have been generated by tidally forced water from the Monterey Bay Canyon coming in contact with the canyon edge; similar to some of Petruncio's (1998) observations. Second, the ITBs could have been generated at the westward continental shelf break, propagated directly shoreward, but then been refracted by the coastline and propagated southward as internal edge waves. If the along-shore current signature was weak and the cross-shore current velocity signature was observed to be consistently strong, then ITB events would most likely have been generated at the westward continental shelf break and shoaled primarily in the cross-shore direction. Statistical and graphical analyses were employed to assess these hypotheses.

V. RESULTS AND DISCUSSION

A. TIDAL AMPLITUDE

One hypothesis was that leading-edge, upper-layer, cross-shore current magnitudes for each event would increase with the barotropic tidal amplitude associated with each event. This relationship would be expected because shelf-break tidal forcing occurs in the cross-shore direction. Additionally, it was hypothesized that the correlation between tidal amplitude and along-shore current magnitude would be less than that of cross-shore magnitude because along-shore magnitude is not parallel to tidal forcing.

Figure 27 shows the regression of tidal amplitude and upper column leading-edge cross-shore current velocities for solibore events. The correlation coefficient, -0.03964, indicates a weak relationship; however, the regression plot indicates that a majority of solibore events occurred when tidal amplitudes were on the order of 1.4 m or greater. The lack of correlation could indicate that a "saturation effect" is occurring at this shallow site. ITBs might be weakly and continuously dissipating as they shoal onshore, so that at the 12 m depth point of observation, the impact of the variation in the offshore barotropic tide is not seen. The regression of current data and tidal amplitude much further offshore would likely yield a more definitive relationship.
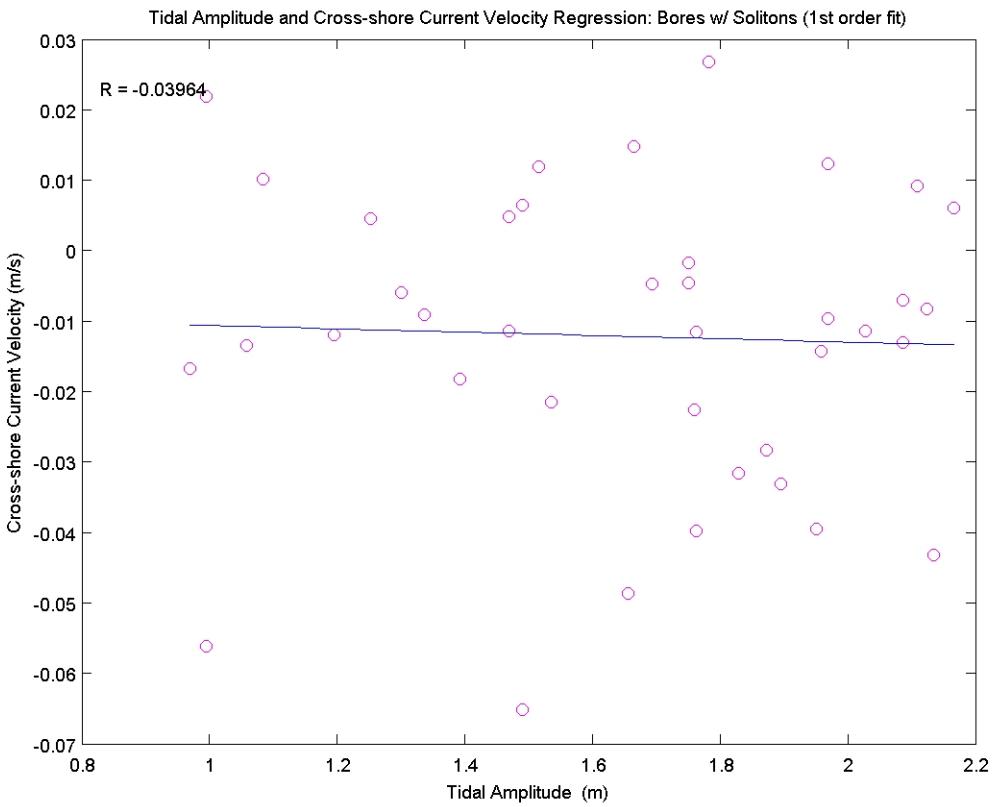
Figure 27.   Solibores: regression of upper column leading-edge cross-shore current
velocities per event and tidal amplitude

The same correlation of tidal amplitude and upper column cross-shore current velocity was completed using only bore events (Figure 28). This correlation showed more significance with a correlation coefficient of 0.4552. Figure 28 shows that at a tidal amplitude of ~2 m, current velocities varied from 0.01 to -0.04 m/s. The ellipse in Figure 28 outlines a cluster of events that illustrate a variety of current magnitudes were observed at similar tidal amplitudes. The regression plot does indicate that most bore events occur when tidal magnitudes are 1.4 m or greater, as did the same regression for solibore events. Although the regression line indicates that current magnitude decreases with increasing tidal amplitude, the four events that occurred near the greatest tidal amplitude (~ 2.4 m) did have cross-shore current magnitudes greater than 2 cm/s. Additionally, while upper column cross-shore velocity for both solibore and bore events

is predominantly negative (onshore), the bore events that occurred near the maximum tidal amplitude had both positive and negative cross-shore signatures, reducing the significance of the correlation.
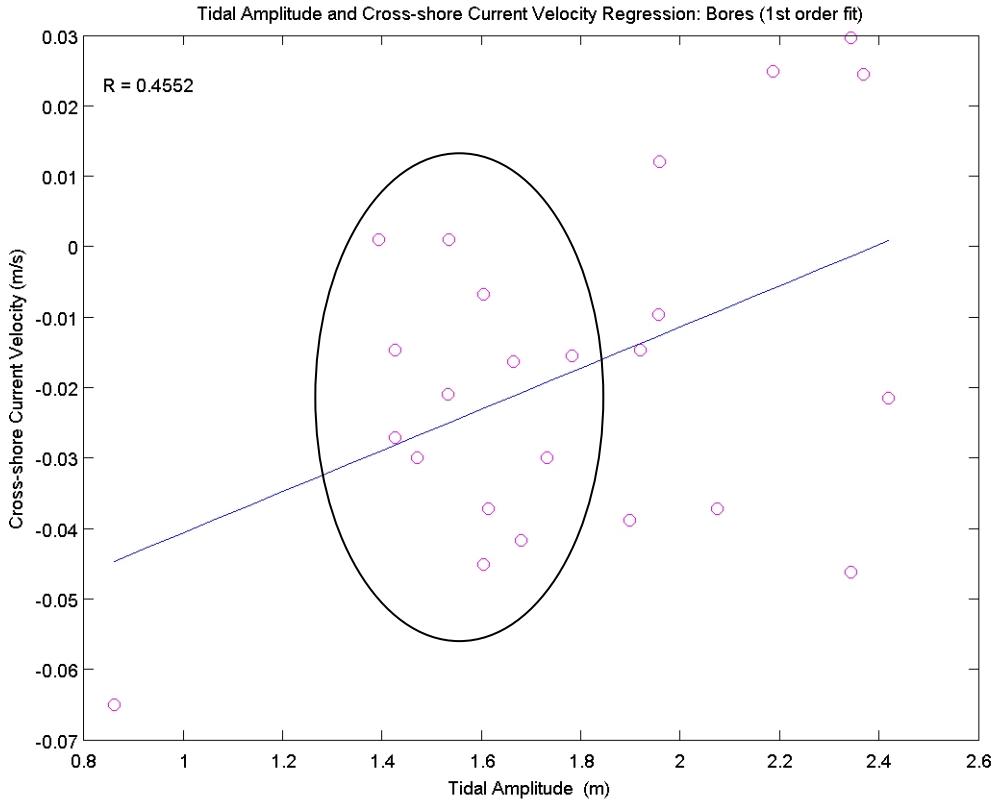
Figure 28.   Bores: regression of upper column leading-edge cross-shore current velocities per event and tidal amplitude. The ellipse marks a cluster of events that indicate tidal amplitude has little effect on cross-shore current velocity magnitude and that most bore events occur when tidal magnitude is 1.4 m or greater.

In the along-shore direction, a regression of upper column solibore current velocities and tidal amplitude produced a correlation coefficient (0.2823) of lesser magnitude than did the same regression in the cross-shore direction. However, because almost all of the along-shore currents are negative and the regression line is positive, an increase in tidal amplitude scales with a decrease in along-shore current magnitude. The decrease in along-shore current magnitude with increased tidal amplitude could be a response to an increase in cross-shore current magnitude with increased tidal amplitude. Generally, however, upper column along-shore solibore current magnitudes, Figure 29,

were greater than their respective cross-shore current magnitudes with a maximum magnitude of 0.16 m/s and a mean magnitude between 0.04 and 0.06 m/s. Along-shore current velocities varied widely with respect to tidal amplitude. Events occurring with a tidal magnitude of 2 m or greater were associated with along-shore currents ranging from -0.06 to 0.02 m/s. No significant data clustering was noted.
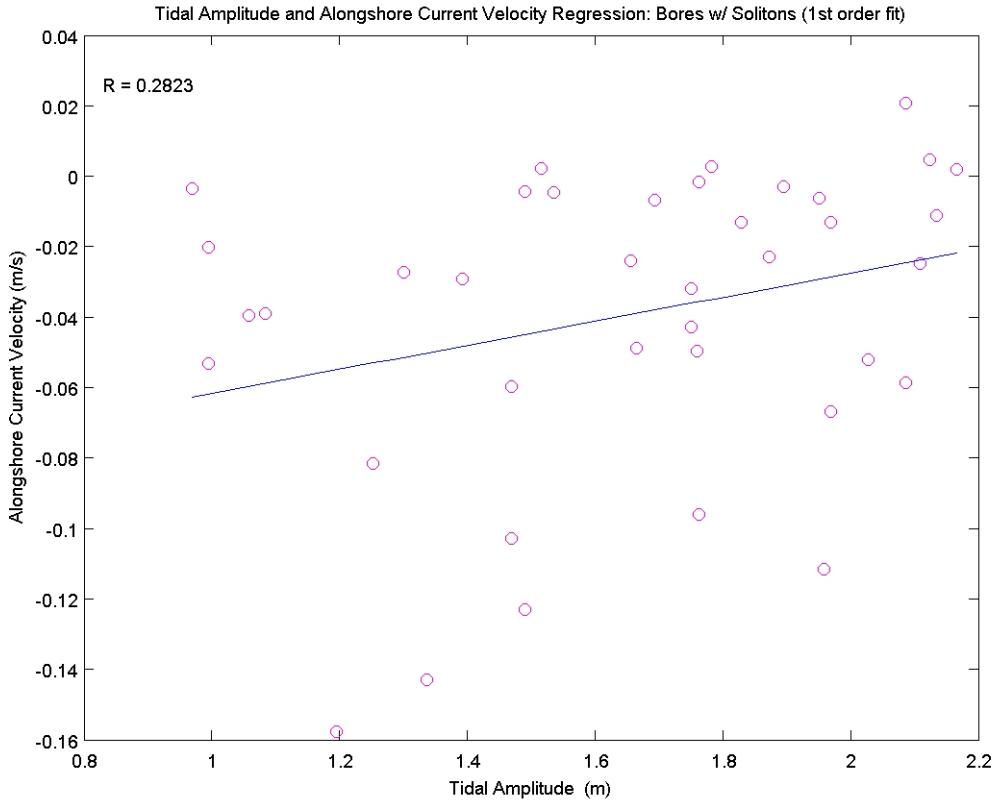
Figure 29.   Solibores: regression of upper column along-shore current velocities per event and tidal amplitude.

A regression of upper column along-shore bore current velocities and tidal amplitude, Figure 30, showed a negative correlation indicating that the magnitudes of the predominantly negative currents did increase with tidal amplitude. The along-shore bore current magnitude and tidal amplitude correlation was indeed less than that of the cross-shore bore current magnitude and tidal amplitude. The ellipse in Figure 30 outlines data showing that at a given tidal amplitude range, upper column along-shore currents varied widely in speed and direction, decreasing the regression magnitude. Leading-edge along-

shore bore currents, with a mean ~ -0.01 to -0.02 m/s, were significantly weaker than the mean solibore along-shore current value of -0.04 to -0.06 m/s.
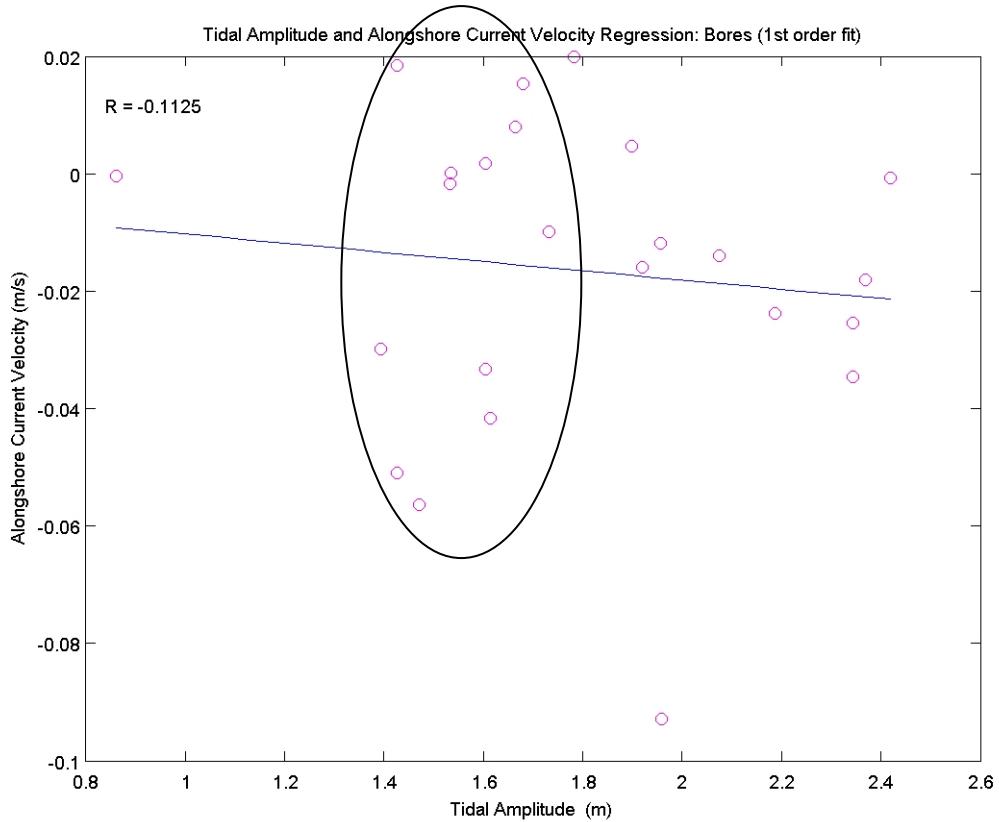
Figure 30.   Bores: regression of upper column along-shore current velocities per event and tidal amplitude. Ellipse outlines data and shows that at a given tidal amplitude, upper column along-shore currents varied widely in speed and direction.

Tidal amplitude regressions showed that solibore and bore events were most likely to occur when tidal amplitude was 1.4 m or greater where the barotropic tidal amplitude reached a minimum of 0.8 m (Figure 13). Both bore and solibore cross-shore and along-shore upper column current velocities were predominantly negative; however, current magnitudes varied widely with respect to tidal amplitude. The hypothesis that increased tidal amplitude yields increased ITB leading-edge current magnitude, especially in the cross-shore direction, was not proven to be true. Finally, observations are limited to 60 days of data. More observations could enhance results.

B.   WINDS

It was hypothesized that winds and leading-edge currents would be positively correlated because strong diurnal afternoon sea breezes are prevalent in Monterey Bay during the summer. It was also hypothesized that the wind/current correlation would be less than that of the tides and event-associated currents because these events are believed to be dominantly tidal-forced. Figure 31 shows the regression of cross-shore winds and leading-edge current velocities of all bore, solibore, and soliton events (significant events). Cross-shore currents were predominantly negative with a mean value ~ -0.01 m/s. The negatively sloped regression line did not support the hypothesis. A correlation coefficient of -0.1708 indicates any relationship was weak and not statistically significant. The small ellipse in Figure 31 outlines events where cross-shore wind magnitudes were the strongest and negative. Furthermore, the small ellipse shows that upper level cross-shore current velocities were predominantly weakly positive during those events. The large ellipse in Figure 31 shows maximum current magnitudes occurred when cross-shore wind magnitude was relatively weak. These observations indicate that cross-shore wind forcing does not significantly impact the leading-edge cross-shore current velocities of ITB events.
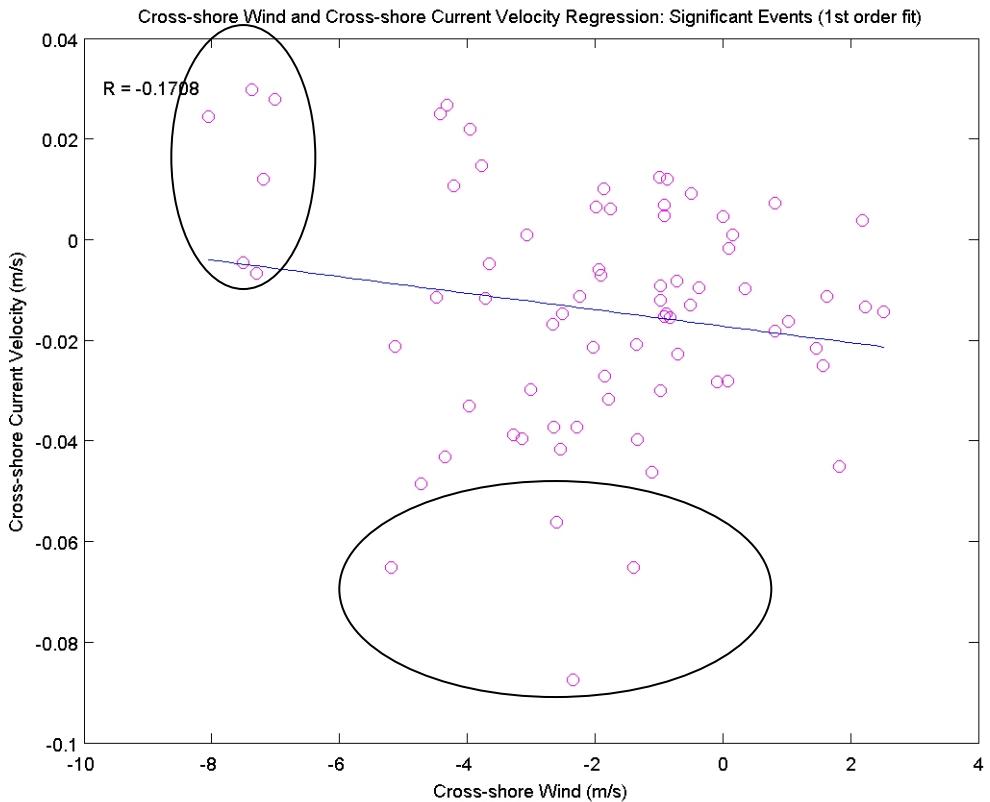
Figure 31.   Significant Events (Bores, Solibores, and Solitons): Upper column leading-edge cross-shore current velocity and cross-shore wind regression. The small ellipse shows that at the greatest cross-shore wind magnitudes, upper level cross-shore currents were of variable direction and weak magnitude. The large ellipse indicates that when the strongest current velocities occurred, cross-shore wind magnitudes were relatively weak.

In the along-shore direction, correlation between winds and leading-edge currents was very weakly positive (R=0.04518) as the hypothesis suggested. The mean along-shore upper column current velocity was ~-0.03 m/s. The small ellipse in the upper portion of Figure 32 shows that a majority of event-associated upper column leading-edge along-shore currents were weakly negative when associated along-shore winds were weakly negative. The large narrow ellipse in Figure 32 shows, however, that when events had the greatest along-shore current magnitudes (> 0.1 m/s), along-shore winds were variable in magnitude and direction. Along-shore wind and event-associated current

analysis indicates that along-shore wind forcing is not a dominant forcing mechanism influencing the along-shore current component at the leading edge of an ITB.
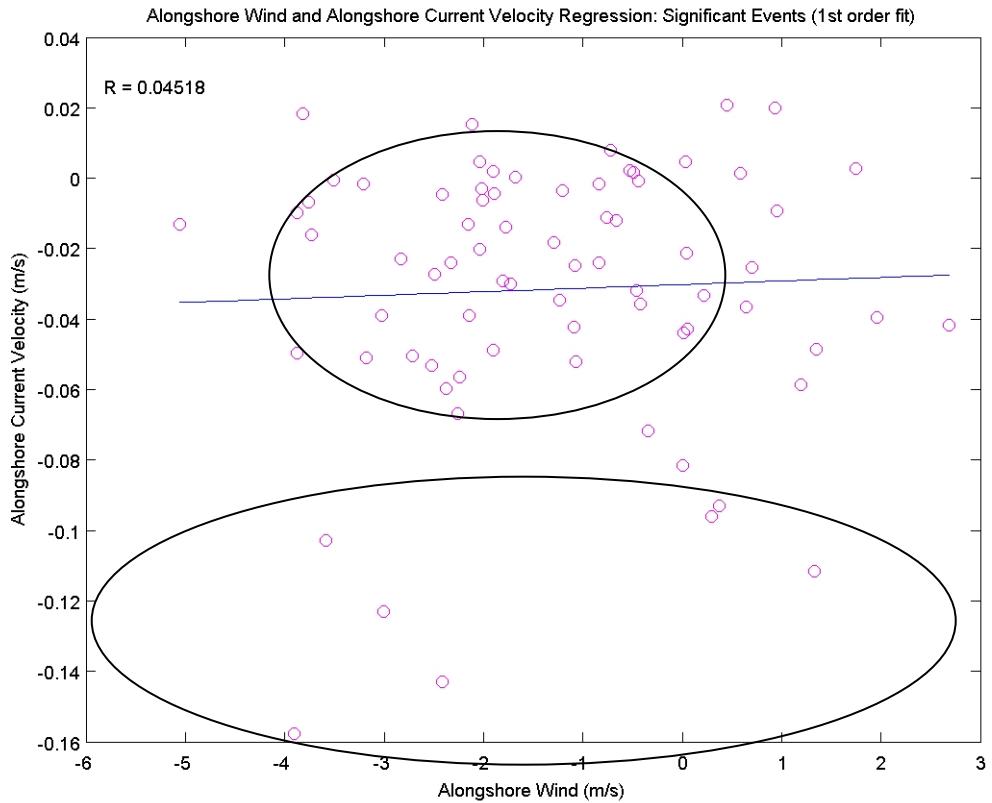
Figure 32.   Significant Events (Bores, Solibores, and Solitons): Upper column leading-edge along-shore current velocity and along-shore wind regression. The small ellipse in the upper portion of the regression plot shows that a majority of event-associated upper column leading-edge along-shore currents were weakly negative when associated along-shore winds were weakly negative. The large narrow ellipse shows that when events had the greatest along-shore current magnitudes (> 0.1 m/s), along-shore winds were variable in magnitude and direction.

C. TRAVEL TIME

If ITB events are generated by a shelf-break lee wave, ebb tide process, then a fairly constant relationship between time elapsed since previous tidal ebb (travel time) and the time an event occurred (event time) would be expected. Variation in arrival time would depend on the stratification-dependent phase speed and generation site distance. An average ITB phase speed of 30 cm/s was calculated using Holloway and Merrifield's (1999) two-layer linear system formula and AUV stratification data from YD 214, 227, and 249 (Figures 7, 8, 9). The phase speed formula for a deep water internal wave in a two-layer system is $c = \sqrt{(g * \Delta\rho * h_1)/\rho_2}$. Here acceleration due to gravity g is 9.8 m/s, surface layer depth is h_1, density contrast between upper and lower layers is $\Delta\rho$, and lower layer density is ρ_2. The average ITB travel time of 11.8 hours was calculated using an approximate distance from the westward continental shelf break to MISO of 12 km (Table 3).

YD	h_1 (m)	ρ_1 (kg/m^3)	ρ_2 (kg/m^3)	$\Delta\rho$ (kg/m^3)	c (m/s)	Travel Time (hrs)
214	12	1024.8	1025.8	1	0.34	10.5
227	10	1024.5	1025.8	1.3	0.35	10.2
249	8	1025.3	1025.8	0.5	0.20	17.8
AVG	10	1024.9	1025.8	0.93	~ 0.3	11.8

Table 3.   Water column characteristics from YD 214, 227, and 249, phase speed calculation and calculation of propagation time from the westward continental shelf break and MISO. The phase speed formula (Holloway and Merrifield 1999) applicable to a deep water internal wave in a two-layer linear system. Distance from shelf break to MISO was approximated to be 12 km.

The upper panel of Figure 33 displays the histogram of travel time and the number of bore events while the lower panel shows the histogram for solibore events. Histogram observations indicate bore and solibore event times vary widely relative to the

tidal ebb times. If the hypothesis was true, data grouping in both panels would be expected near 0 and 12 hours post-tidal ebb with null values in between the two groupings. A null is seen in the top panel of Figure 33 at 6 hours post-ebb time; however, event times are not specifically grouped at 0 and 12 hours post-ebb time. In the lower panel of Figure 33, there are no dominant travel times with an even spread across the histogram.

ITB events observed at MISO could have been generated in different locations which would make the shelf-break lee wave generation process difficult to test. Wave phase velocity variability due to stratification and depth changes across the shelf of bore and solibore event travel times will also blur travel times across the shelf. While the deep water two-layer linear system internal wave speed formula is applicable for a majority of the ITB events' propagation paths across the Monterey Bay shelf, it is not correct for the highly non-linear ITB events in the shallow inner-shelf environment. Data sets with more observation points across the shelf would more clearly define generation sites.
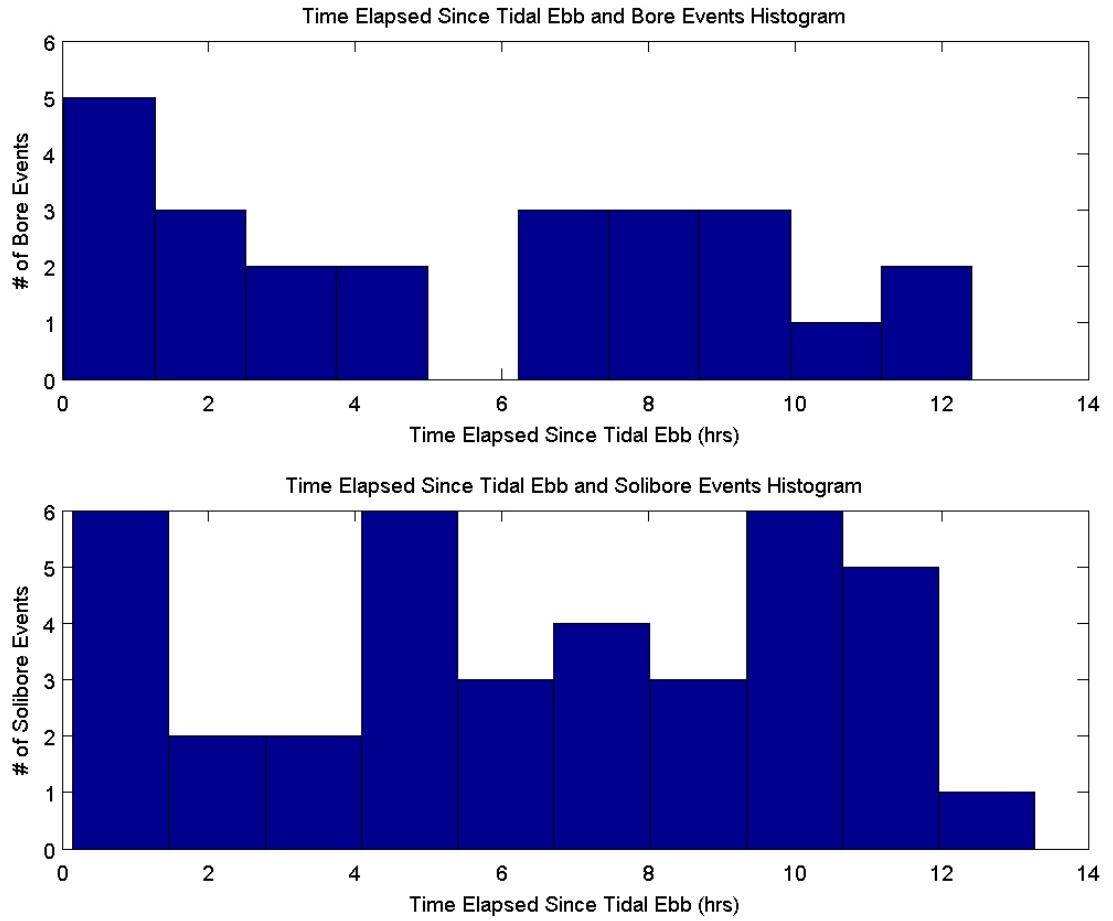
Figure 33.   Top panel: histogram of bore events and time elapsed from tidal ebb (travel time). Bottom panel: histogram of solibore events and travel time.

D.   INTERNAL TIDAL BORE CURRENT VECTOR PLOTS

ITB events may propagate directly shoreward from the western continental shelf-break, southward from a generation point associated with the Monterey Bay Submarine Canyon, or southward as a coastally-guided internal edge wave. Current vector plots were generated to test directionality hypotheses. Different event classifications were used to more fully observe leading edge current characteristics.

1. Significant Events

Significant events include all bore, solibore, and soliton events. Figure 34 displays the current vector plot of significant events. In the top panel of Figure 34, upper column leading-edge current velocities are plotted for each event. In the bottom panel, lower column leading-edge current velocities are plotted for each event. A red asterisk marks the mean cross-shore and along-shore velocity of all of the events shown. In this case, it is shown that net lower column motion is indeed weakly in the offshore direction. The top panel of Figure 34 confirms that the measured along-shore current associated with ITB events is predominantly negative, or towards Monterey, and mean upper column cross-shore motion is onshore. These findings indicate that the ITB events observed at MISO are significant onshore pulses of water in the upper column and strong offshore pulses in the lower column. The predominantly negative along-shore velocity in the upper column indicates that ITB events do not propagate directly onshore from a generation site at the westward shelf break, but that the coastline and/or the Submarine Canyon may impact ITB current velocities.
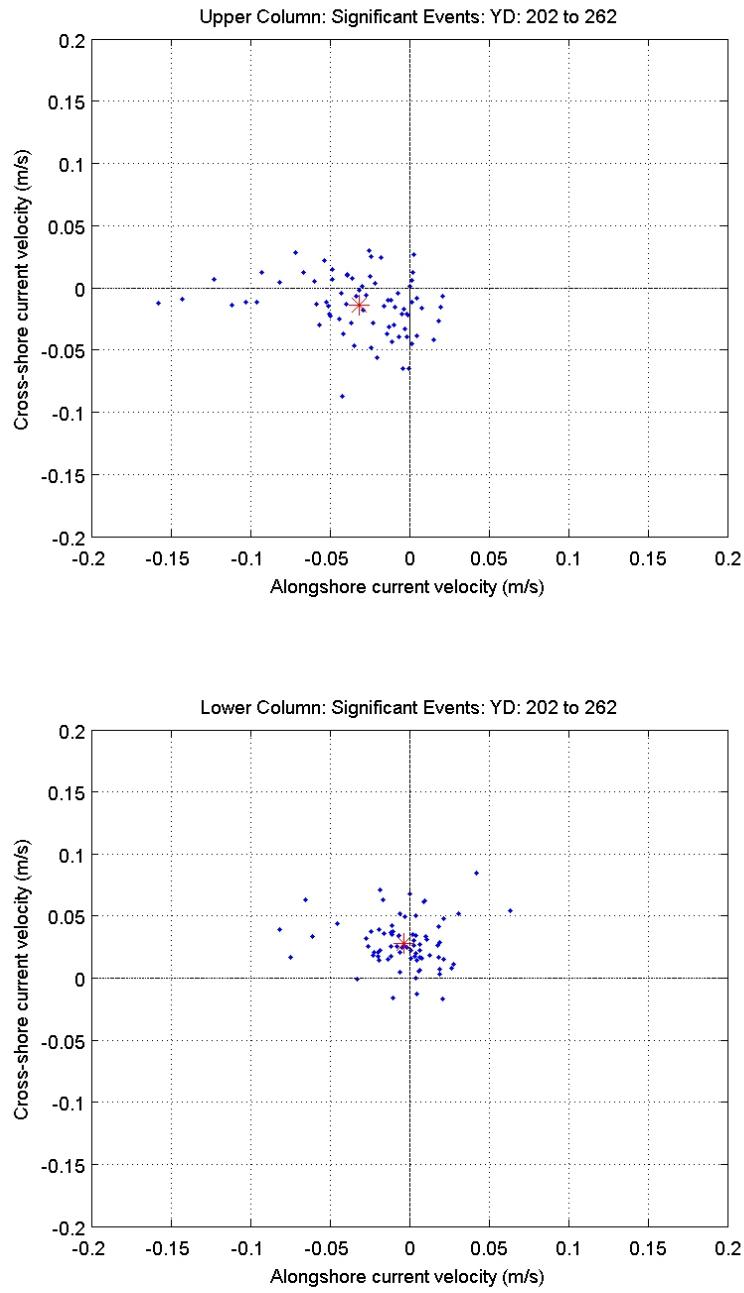
Figure 34.   Event vector plot of all significant events. Top panel is upper column leading-edge sampled current velocities per event and the bottom panel represents those of the lower column. Each velocity is an average representing an individual event. The red asterisk marks the mean velocities of all of the events shown.

63

2. Bore Events

The same hypotheses regarding event current vectors were applied solely to bore events. Findings were similar, Figure 35. Net offshore motion was seen in the lower column. Upper column along-shore motion was predominantly negative, or towards Monterey while upper level cross-shore motion was onshore.
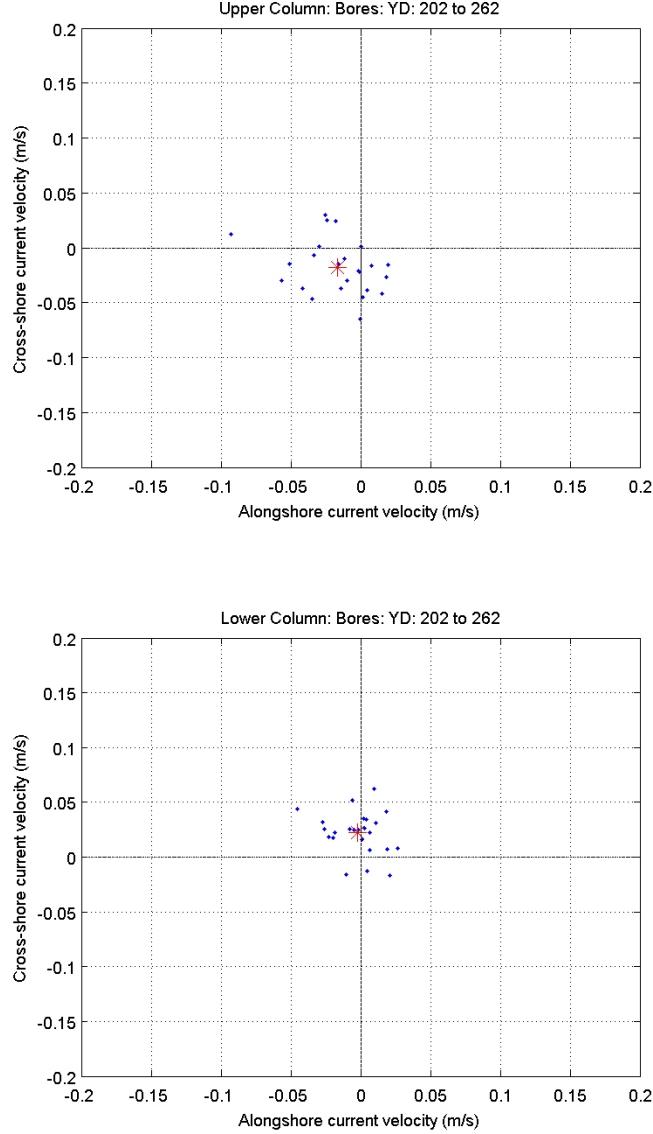
Figure 35.   Event vector plot of all bore events. Top panel is upper column leading-edge current velocities per event and bottom panel is lower column leading-edge current velocities. Each velocity is an average representing an individual event. The red asterisk marks the mean velocities of all of the events shown.

3. Solibore Events

Solibore events were analyzed separately to observe leading-edge current vector patterns. The findings in this case were very similar to those of the significant events and bore testing. However, in this case, all lower column cross-shore velocities were measured to be zero or offshore; no negative outliers were observed (Figure 36). Upper column along-shore velocities were also more highly skewed to the negative direction (see the ellipse in Figure 36) than were the bore current vectors. These definitive patterns may be attributed to the current sampling occurring in the solitons which are the highest energy portion of the ITB event. High energy events in the negative along-shore direction indicate that ITBs are either initially moving in the along-shore direction or that through shoaling and refractive processes ITB energy is transferred to the along-shore direction.
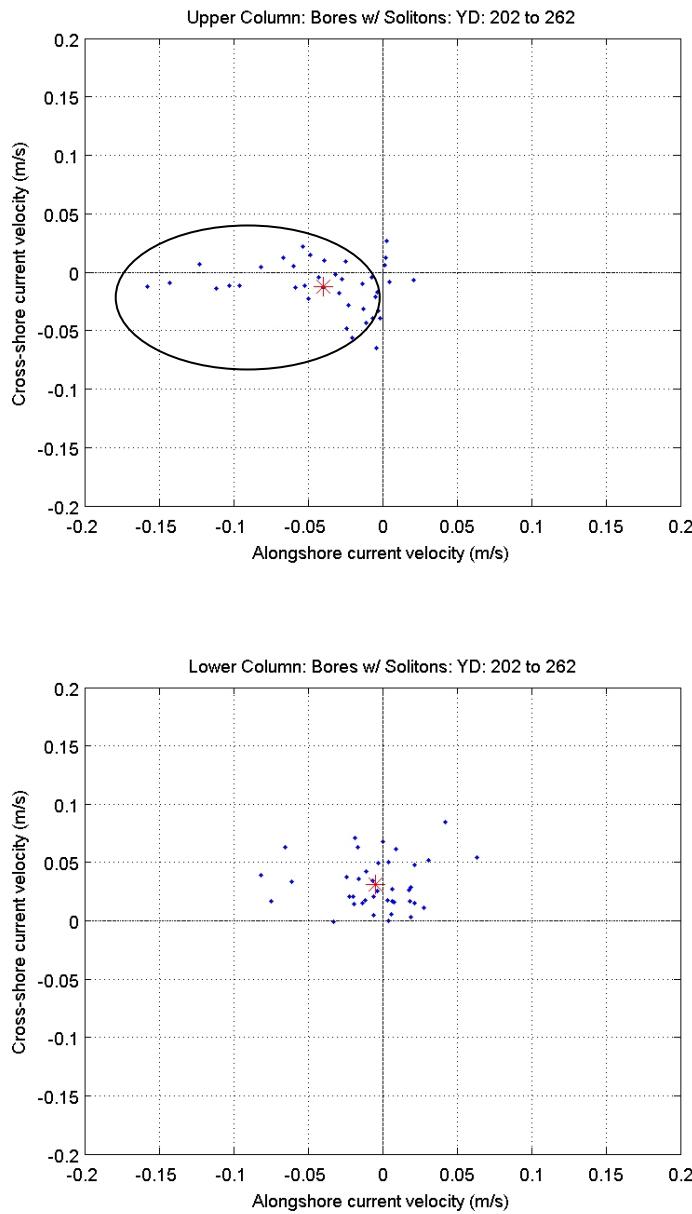
Figure 36.   Event current vector plot of all solibore events. Top panel is upper column leading-edge current velocities per event and the bottom panel is those of the lower column. Each velocity is an average representing an individual event. The red asterisk marks the mean velocities of all of the events shown. The ellipse in the top panel outlines predominantly negative along-shore current signature data points.

4. Soliton Events

The event vector plot of soliton events, Figure 37, is most closely related to the solibore current vector plot. All lower column cross-shore currents are onshore. Additionally, all of the along-shore current velocities associated with the leading edge of each soliton event are negative. This finding supports the conclusion that the most highly energetic ITB events have substantial along-shore components that are predominantly negative, or towards Monterey.
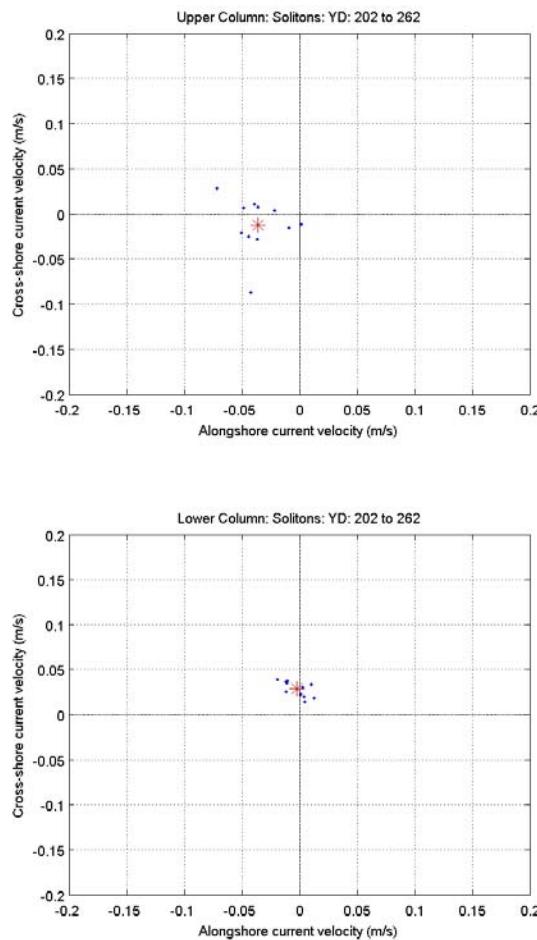

Figure 37.   Wave spectra plot of all soliton events. Upper panel is upper column current velocities and lower panel is lower column current velocities. Each velocity is an average representing an individual event. The red asterisk marks the mean velocities of all of the events shown.

THIS PAGE INTENTIONALLY LEFT BLANK

VI. CONCLUSION

A. INTERNAL TIDAL BORE CHARACTERISTICS

No significant pattern was found to associate ITB events of one shape, duration, or maximum excursion to another; however, several characteristics were similar to all of the bores observed at MISO. First, ITB events depend strongly on two main factors: stratification and forcing. AUV and MISO data showed that near-surface stratification across the shelf and a barotropic tidal amplitude greater than 1.4 m had to be present before ITB events were detected. Second, all of the ITB events could be classified into three categories: bore, solibore, or soliton events. Third, all of the bores were characterized by their steep isotherm excursions. ITB excursions extended downward from ½ of the water column through the entire water column. Fourth, all of the events produced net upper column leading-edge onshore current transport, net lower column leading-edge offshore current transport, and predominantly negative upper column along-shore current transport. Fifth, it was determined that ITB events are best characterized by their leading edges because of the strong current signature located there. Strong mode 1 velocity fluctuations characterized the leading edge of all ITB events; particularly, the steepest and most energetic soliton and solibore events. While these events were the most challenging to sample, their complex but observable signatures provided very specific information regarding the leading-edge current vector patterns of events. Finally, it was shown that neither tidal amplitude nor wind velocity directly control the leading-edge velocity of an ITB at the inner shelf site. This finding could be attributed to the shoaling and dissipation of the ITBs as they traversed the shallowing inner shelf. Table 4 shows a synopsis of the regressions completed to assess these relationships.

ITB Data:	Tidal Amp vs. CS current	Tidal Amp vs. AS current	CS wind vs. CS current	AS wind vs. AS current
Bore Events	0.4552	-0.1125	-0.5735	-0.2513
Soliton Events	-0.3853	0.1149	-0.1472	0.3422
Solibore Events	-0.03964	0.2823	0.159	0.1404
All Significant Events (Excludes Weak Events)	0.03487	0.1983	-0.1708	0.04518

Table 4.   Correlation coefficients of various regressions and specific portions of data.

B.   LEADING-EDGE CURRENT VECTORS

MISO observations contributed to several findings. All bore, solibore, and soliton events seen at MISO created net offshore flow in the lower water column. These offshore flows may contribute to bed reformation or sediment transport. The strength of the offshore flow may also be a helpful indicator of the strength of the event. Stronger offshore flow in the lower column indicates stronger onshore flow in the upper column. Upper column cross-shore flow was predominantly negative or onshore which was expected as per previous ITB research. Upper column along-shore flow was predominantly negative in all cases. This indicates that ITB events are approaching MISO from the direction of Marina and moving towards Monterey. If events were coming from the shelf break directly westward, along-shore motion would most likely be minimal in comparison to cross-shore motion. This assessment found that not only was along-shore leading-edge current velocity predominantly negative in the upper column, but that along-shore event velocities were also generally greater in magnitude than cross-shore current velocities. This assessment concludes that ITB events recorded at MISO are most likely being generated at the Monterey Bay Submarine Canyon or are cross-shore events that reach the coastline, refract, and propagate southward as an internal edge wave.

C.   NAVAL IMPACT

This research is a step towards understanding the highly complex nearshore environment and how bathymetric features like submarine canyons and shelf breaks can

be generation sites for tidally forced features. ITB research is particularly pertinent to several coastlines of strategic military interest including the Chinese and Korean coastlines. High amplitude internal disturbances like internal tidal bores make military special operations difficult. Specific operational risks include SEAL Delivery Vehicle operations, amphibious landings, and mine warfare. This research contributes to the understanding of coastal oceanographic water column disturbances of which expanded knowledge could increase safety for littoral operators, improve knowledge of the coastal acoustic environment, and enhance nearshore model resolution. Models including the "saturation effect" found in the inner shelf environment may increase model effectiveness.

D.   FUTURE RESEARCH

Future research suggestions include analyzing data from other ADCPs in the Monterey Bay; particularly those in Sand City and Marina. Deploying more ADCPs and thermistors along the Monterey Bay coastline and along the Submarine Canyon would also provide data useful for determining a dominant ITB generation site. An increased number of observation sites could indicate whether the negative along-shore leading-edge current velocities of ITB events observed at MISO are due to propagation from the canyon, to internal edge wave propagation along the coast, or to a process not discussed here. Further analysis of the wind-current and tide-current relationships to the strength of ITB events could further characterize ITB events.

THIS PAGE INTENTIONALLY LEFT BLANK

LIST OF REFERENCES

Alpers, W., L. Mitnik, L. Hock, and K.S. Chen. (updated March 21, 2002). *The tropical and subtropical ocean viewed by ERS SAR.* Retrieved February 20, 2007, from http://www.ifm.uni-hamburg.de/ers-sar/Sdata/oceanic/intwaves/intro/index.html.

Apel, J.R., J.R. Holbrook, J. Tsai, and A.K. Liu, The Sulu Sea internal soliton experiment, *Journal of Physical Oceanography,* 15 (12), 1625-1651, 1985.

Baines, P.G., On internal tide generation models, *Deep Sea Research*, 29, 3A, 307-338, 1982.

Blumberg, A.F., and G.L. Mellor, A Description of the Three-Dimensional Coastal Ocean Circulation Model: *in* Heaps, N.R., ed., *Coastal and Estuarine Sciences 4*: American Geophysical Union, 1-15, 1987.

Farmer, D., and L. Armi, The generation and trapping of solitary waves over topography, *Science*, 283, 188-190, 1999.

Garrett, C., Ocean Science: Internal Tides and Ocean Mixing: *Science Week*, 301, 1858-1859, 2003.

Garrett, C., Internal Waves: *in* Steele, J., Turekian, K. and Thorpe, S., eds., *Encyclopedia of Ocean Sciences*, 3, 1335-1342, 2001.

Garrett, C., and W. Munk, 1979, Internal Waves in the Ocean: *Annual Review of Fluid Mechanics*, 11, 339-369, 1979.

Holloway, P.E., and M.A. Merrifield, Internal tide generation by seamounts, ridges, and islands, *Journal of Geophysical Research*, 104, C11, 25, 937-25, 951, 1999.

Holloway, P.E., Internal Hydraulic Jumps and Solitons at a Shelf Break Region on the Australian North West Shelf, *Journal of Geophysical Research,* 92, C5, 5405-5416, 1987.

Hosegood, P. and H. van Haren, Near-bed solibores over the continental slope in the Faeroe-Shetland Channel, *Deep Sea Research II*, 51, 2943-2971, 2004.

Klymak, J.M., R. Pinkel, C. Liu, A.K. Liu, and L. David, Prototypical solitons in the South China Sea, *Geophysical Research Letters*, 33, L11607, 2006.

Kropfli, R.A., Ostrovski, L.A., Stanton, T.P., Skirta, E.A., Keane, A.N., and V. Irisov, Relationships between strong internal waves in the coastal zone and their radar and radiometric signatures, *Journal of Geophysical Research,* 104, C2, 3133-3148, 1999.

Kuperman, W.A. and J.F. Lynch, Shallow Water Acoustics, *Physics Today*, 2005, online accessed, www.physicstoday.org, February 2007.

Lee, Ch-Y. and R.C. Beardsley, The generation of long nonlinear internal waves in a weakly stratified shear flow. *Journal of Geophysical Research*, 79, 453-457, 1974.

Marine Measurements Group of Teledyne RD Instruments. (n.d). *Workhorse Monitor ADCP.* Retrieved January 28, 2007, from http://www.rdinstruments.com/monitor.html.

MBARI AUV Project Leaders. (updated March 13, 2007). *Autonomous Underwater Vehicles.* Retrieved February 7, 2007, from http://www.mbari.org/auv.

Mullen, M.G., *Chief of Naval Operations.* Retrieved February 7, 2007, from http://www.navy.mil/navydata/leadership/ldrDisplay.asp?m=11.

Munk, W., Internal Tidal Mixing: *in* Steele, J., Turekian, K. and Thorpe, S., eds., *Encyclopedia of Ocean Sciences*, 3, 1323-1326, 2001.

Petruncio, E.T., Observations of the Internal Tide in Monterey Canyon, *Journal of Physical Oceanography,* 28, 1873-1903, 1998.

Pike, J. (updated July 30, 2005). *Seal Delivery Vehicle [SDV].* Retrieved February 8, 2007, from http://www.globalsecurity.org/military/systems/ship/sdv.htm.

Ray, R.D., Internal Tides: *in* Steele, J., Turekian, K. and Thorpe, S., eds., *Encyclopedia of Ocean Sciences*, 3, 1327-1335, 2001.

Stanton, T.P. (1998). *Rapid Environmental Assessment Laboratory (REAL): Monterey Inner Shelf Observatory (MISO).* Retrieved January 16, 2007, from http://www.oc.nps.navy.mil/~stanton/miso.

Stanton, T.P., and L.A. Ostrovsky, Observation of highly nonlinear internal solitons over the continental shelf, *Geophysical Research Letter*, 25, 14, 1998.

Tjoa, K.M, The bottom boundary layer under shoaling inner shelf solitons, Master's Thesis, Naval Postgraduate School, 2003.

Wunsch, C., Moon, tides, and climate, *Nature,* 405, 743-744, 2000.

INITIAL DISTRIBUTION LIST

1. Defense Technical Information Center
    Ft. Belvoir, Virginia

2. Dudley Knox Library
    Naval Postgraduate School
    Monterey, California

3. Dr. Donald P. Brutzman
    Naval Postgraduate School
    Monterey, California

4. Dr. Mary L. Batteen
    Naval Postgraduate School
    Monterey, California

5. VADM Roger Bacon, USN (Ret.)
    Naval Postgraduate School
    Monterey, California

6. CDR Denise Kruse, USN
    Naval Postgraduate School
    Monterey, California

7. Dr. Daphne Kapolka
    Naval Postgraduate School
    Monterey, California

8. Dr. Timothy Stanton
    Naval Postgraduate School
    Monterey, California

9. Dr. William Shaw
    Naval Postgraduate School
    Monterey, California

10. Mr. James Stockel
    Naval Postgraduate School
    Monterey, California

11. LT Sarah Heidt, USN
    Naval Postgraduate School
    Monterey, California

12.   ENS Rebecca Wolf, USN
Naval Postgraduate School
Monterey, California

13.   CDR Emil Petruncio, USN
United States Naval Academy
Annapolis, Maryland

14.   LT Nathan Gammache, USN
Naval Postgraduate School
Monterey, California

15.   Major Joseph Delaney, USMC
Naval Postgraduate School
Monterey, California

16.   ENS Kendra Crabbe, USN
Naval Postgraduate School
Monterey, California